

Copyright Warning & Restrictions

The copyright law of the United States (Title 17, United States Code) governs the making of photocopies or other reproductions of copyrighted material.

Under certain conditions specified in the law, libraries and archives are authorized to furnish a photocopy or other reproduction. One of these specified conditions is that the photocopy or reproduction is not to be “used for any purpose other than private study, scholarship, or research.” If a user makes a request for, or later uses, a photocopy or reproduction for purposes in excess of “fair use” that user may be liable for copyright infringement,

This institution reserves the right to refuse to accept a copying order if, in its judgment, fulfillment of the order would involve violation of copyright law.

Please Note: The author retains the copyright while the New Jersey Institute of Technology reserves the right to distribute this thesis or dissertation

Printing note: If you do not wish to print this page, then select “Pages from: first page # to: last page #” on the print dialog screen

The Van Houten library has removed some of the personal information and all signatures from the approval page and biographical sketches of theses and dissertations in order to protect the identity of NJIT graduates and faculty.

ABSTRACT

INTERVENTIONS OF WATER JET TECHNOLOGY ON SKIN SURGERY

**by
Kittipat Vichyavichien**

The perfect and precise surgical cut, similar to today's laser one, is very important in many surgeries, especially in dissection and to recanalize arterial occlusive lesions. Causing no coagulation is one of the advantages of water jet because it generates no heat. It also provides omni-directional cutting capabilities at very high speeds, resulting edge quality that is usually superior to other existing conventional cutting processes. Debris is always carried away from incisions by jet stream and less damaged tissue than mechanical incisions. In addition, water jet exerts minimal contact pressure on the tissue being cut due to the small diameter of jet stream. It decreases the degree of distortion and more precise incisions acquired. A total number of 48 computational nonlinear analyses are carried out using finite element method to find the effects of water jet on skin layers and behavior of skin layers under pressures. The sensitivity analysis was conducted to compare among performance values in terms of width and depth of cut. The results obtained show linear effect that is elastic behavior. The skin material ruptures before going into the plastic region and start to shear at the pressure of 40MPa with the 0.2mm nozzle. The epidermis absorbs most of the stress and is deformed while other layers are also slightly deformed but do not reveal high stress concentration. The exact equations governing the interaction of high velocity water jet and the skin material are complex and detailed.

**INTERVENTIONS OF WATER JET TECHNOLOGY
ON SKIN SURGERY**

by
Kittipat Vichyavichien

**A Thesis
Submitted to the faculty of
New Jersey Institute of Technology
in Partial Fulfillment of the Requirement for the Degree of
Master of Science in Manufacturing Systems Engineering**

Department of Industrial and Manufacturing Engineering

August 1999

APPROVAL PAGE

**INTERVENTIONS OF WATER JET TECHNOLOGY
ON SKIN SURGERY**

Kittipat Vichyavichien

Dr. George Hanna Abdou, Thesis Advisor Date
Associate Professor of Industrial and Manufacturing Engineering, NJIT

Dr. Carl Wolf, Committee Member Date
Professor of Industrial and Manufacturing Engineering, NJIT

Dr. One-Jang Jeng, Committee Member Date
Associate Professor of Industrial and Manufacturing Engineering, NJIT

BIOGRAPHICAL SKETCH

Author: Kittipat Vichyavichien

Degree: Master of Science

Date: August 1999

Undergraduate and Graduate Education:

- Master of Science in Manufacturing Systems Engineering,
New Jersey Institute of Technology, Newark, New Jersey, 1999
- Bachelor of Engineering in Mechanical Engineering,
King Mongkut Institute of Technology at Lardkrabang, Bangkok, Thailand, 1995

To my beloved family

ACKNOWLEDGMENT

The author wishes to express his deep appreciation and sincere gratitude to his advisor, Dr George Abdou for his patiently guidance, understanding and generous friendship throughout the research. This thesis would have been failed unless helped from his contribution.

The author also extends his gratitude to Dr. Carl Wolf and Dr. One-Jang Jeng for serving as members of the thesis committee.

Special thanks to William Tereshkovich, Nitipong Boon-long, and Akintayo Adewole for their helps in starting the research, and very useful suggestions during the research.

In addition, the author would like to pay a special tribute to his parents, brother for all of their unconditional love and support.

TABLE OF CONTENTS

Chapter	Page
1. INTRODUCTION	1
1.1 Water Jet Cutting Capabilities	1
2. LITERATURE REVIEW	3
2.1 Experiments on Actual Soft Tissues	3
2.2 Finite Element Analysis of Skin Models	9
2.3 Limitations	10
3. OBJECTIVES AND PROCEDURES	12
4. FRAME WORK OF WATER JET CUTTING ON SKIN	13
4.1 Water Jet and its Operating Parameters	13
4.1.1 Operating Parameters	14
4.2 Structure and Mechanical Properties of Skin	17
4.2.1 Skin Components and Mechanical Roles	18
5. PROPOSED METHODOLOGY	20
5.1 Finite Element Modules	20
5.1.1 Linear Static Analysis	21
5.1.2 Nonlinear Static Analysis	22
5.2 I-DEAS (Finite Element Analysis Module)	27
5.3 Modules of Modeling/Analysis	27
5.3.1 Geometric Modeling	27
5.3.2 Meshing Modules	29
5.3.3 Model Verification	30

TABLE OF CONTENTS
(Continued)

Chapter	Page
5.3.4 Analysis Modules	31
5.3.5 Post Processing	32
5.4 Design of Experiments	32
5.5 Curve Fitting Using TableCurve Software	35
6. CASE STUDY AND RESULTS	36
6.1 Assumptions	36
6.2 FEA Modeling of Skin	36
6.2.1 Geometric Modeling	36
6.2.2 Boundary Condition	37
6.2.3 Element Modeling	38
6.3 Element and Material Properties	43
6.4 Results	43
7. ANALYSIS OF RESULTS	51
8. CONCLUSIONS AND RECOMMENDATIONS	53
APPENDIX A Results of the Analysis	55
APPENDIX B Results of Elements Verification	66
APPENDIX C I-DEAS Output File (*.lis)	77
GLOSSARY	91
REFERENCES	92

LIST OF TABLES

Table		Page
4-1	Cutting parameters of water jet	14
5-1	Classification of non-linear analysis and governing equations	24
5-2	Design of experiments running with numbers under different cutting parameters	34
6-1	Numbers of elements and the bias numbers along each side	41
6-2	Element types and meshing methods created on the each layer	42
6-3	Mechanical properties of the skin layers and gap element	42
6-4	Extended radius of cut and the depth of cut	43
6-5	Results based on the sizes of the nozzles	44
7-1	Equations of relationship between cutting parameters	51

LIST OF FIGURES

Figure		Page
4-1	Cutting parameters and its components	15
6-1	The skin model	39
6-2	The effective radius	41
6-3	The relationship between the pressure and the maximum shear stress based on the nozzle sizes.	45
6-4	The relationship between the pressure and the displacement based on the nozzle sizes.	45
6-5	The relationship between the pressure and the extended radius of cut	46
6-6	The relationship between the pressure and the depth of cut based on the nozzle sizes	46
6-7	The contour plot of stress distribution	47
6-8	The contour plots of displacement and deformation	48
6-9	The contour plots of area of contact stress and contact pressure	49
6-10	The contour plot of area from 5MPa to 10MPa	50
7-1	The fitted curve equation of radius and depth	52

CHAPTER 1

INTRODUCTION

A narrow water jet at high velocity from a small-diameter (0.03-0.5mm) hole is proven to generate sufficient force for various materials to break microscopic material particles off its main bulk. These properties of water jets motivated researchers of different countries around the world to develop machining methods in which the stream of jet kinetic energy is transformed into mechanical work for cutting or removing particles from subjects. Generally, when the jet stream is utilized as a cutting tool, the velocity of the jet reaches the supersonic region.

Successful studies of water jet in different materials have been undertaken in the United States, Great Britain, Germany and Japan etc. Water jet can be used for the cutting of paper, board, cloth, wood, leather, rubber, plastic or even ceramic materials. The water jet was first patented by the staff of McCartney Manufacturing Company; a division of the Ingersoll-Roland Corp., An experiment machine utilizing this method has been successfully used for cutting various materials since 1971.

1.1 Water Jet Capabilities

The cutting capabilities of water jet depend on a number of factors including the type of material, the composition of the medium (working fluid), the method of cutting and the direction of the water jet with respect to the material surface. Low-strength materials are easier to cut. They require lower pressure. For instance, 200MPa pressure is used in order to cut thin plywood, leather, or rubber. 200-500MPa is used to cut plastics.

Water jet can also be performed for application other than cutting, For example, in considering water jet for surgery uses, it has been introduced into surgical practices by Papachristou and Barthers(1982) for hepatic resections in conventional open surgery and has since been used for this purpose in a numbers of centers during open surgical operations surgical tool. Sohn and Weinstein(1977), used the pulsating water jet to efficiently care and debride the wounds. Water jet is a non-contact cutting tool that means it can cut the soft tissue with generating remarkably less distortion than conventional surgical blades. The cut is precise and shown a fine delineation. The more studies have been done the more advantages of water jet found. The advantages of water jet include simplicity of device, low maintenance cost, clean cutting, and reproducibility.

Because of the limitation of skin models and the complexity of the experimental systems, an analytical approach (such as finite element model) is the best way to investigate practical problems. With a conceptually sound model, based on reasonable estimate of the mechanical properties, Mathematical experiments in skin surgery can be quickly and easily performed. Because of its ability to deal with very complex geometry, Finite element analysis has potential applications in many areas of simulating the problem more accurate enough and closes the gap between models and in vivo samples.

CHAPTER 2

LITERATURE REVIEW

Researches in water jet have been conducted in many aspects. Water jet for surgical is one of the most interesting studies. From heterogeneous and coarser tissues like facial skin to parenchymal organs like livers and brains are taken to be the test subjects. Only few studies specially focused on skin cutting using water jet. Some studies that have been found concerning to this research are reviewed as follow.

2.1 The Experiments Done on Actual Soft Tissues

Siegert R, et al. (1998) used water jet cutter to thin subcutaneous¹ tissue down to 0.4 mm. Findings demonstrated that the method used could create a well-vascularized skin flap of minimal thickness that could be very helpful for special reconstructive procedures, like auricular² reconstruction. This research supports that water jet is safe enough for using for surgery.

Une Y, et al. (1996) used water jet scalpel in hepatic resection were used in two groups of 36 patients with hepatocellular carcinoma. The first group included patients with HCC associated with liver cirrhosis and the second group included patients without cirrhosis. No significant difference in total blood loss, operation times and postoperative complications were noted. The parenchyma³ of the cirrhotic liver was divided but the intrahepatic vessels were spared.

¹ Being, living, used, or made under the skin

² An epithelial parenchymatous cell of the liver

³ The essential and distinctive tissue of an organ or an abnormal growth as distinguished from its supportive framework

In order to avoid laparotomy⁴ in patients with superficially and/or anatomically favorably located liver lesions⁵. Schob OM, et al. (1994) has used laparoscopic⁶. Liver resection using water jet dissector from AQUATOM[®], Medinorm AG. This machine enables the dissection of liver tissue without injury to the intraheptic vessels that allows us to simplify and control the bleeding from cut surface. Using a pump to drive a jet of 0.9% saline. A pressure at 1.7bar was used (pressure capability range: 0.5-10bar). The experiment was evaluated in 6 pigs to dissect the livers. The results were concluded that there were no severe complications such as bleeding or any infections and loss of hematocrit⁷ was acceptable. The liver parameters were normal after a moderate increase at day one due to the trauma of operation. It is obvious that the magnitude of cutting pressure for cutting parenchymal tissue doesn't has to be a very high pressure. The strength of this tissue is significantly less than structural tissues like skins or muscles.

Hubert J, et al. (1996) used the pig models. The experiment was conducted ex vivo (14 kidneys) and in vivo to compare electric cutlery section with water jet dissector. Ex vivo study confirmed sparing of blood vessels and pelvicaliceal system. In vivo study did not show significant differences in blood loss but the water jet allowed precise dissection and tight closure of the excretory system.

Rau HG, et al. (1996) conducted an experiment to compare the end results between ultrasonic aspirator and water jet cutter in terms of Speed of resection, blood loss, transfusion rate, liver hills clamping time and tissue damage, in the liver resections of 60 patients. Water jet cutter was significantly faster with a resection time of 0.35

⁴ Surgical section of the abdominal wall

⁵ Abnormal change in structure of an organ or part due to injury or disease

⁶ A fiber optic instrument inserted through an incision in the abdominal wall and used to examine visually the interior of the peritoneal cavity

⁷ The ratio of the volume of packed red blood cells to the volume of whole blood

min/cm² with less blood loss of 18.4 ml/cm² ($p < 0.05$). Tissue damage was comparable with both techniques.

Penchev RD, et al. (1998) developed a new bimodular jet-cutter “Parenchimoto-01” had successfully performed 11 liver resections, 14 holecystectomies, and 2 lavages of the common bile duct on 25 patients. Decreasing in blood loss, operative time, rate of complications, and length of hospitalization were noted.

Terzis AJ, et al. (1989) conducted an experiment to find the optimal parameters for the water jet cutting system and the histologic⁸ effects in brain tissues. A prototype of water jet cutting system for medical use was developed with 3 sizes of nozzle. The diameters are 0.1mm, 0.2mm, and 0.4mm for nozzle, No.1, No.2, and No.3 respectively. The pressure was varied from 0.5bar–5.0bar with the increment of 0.5bar. The cuts were done with the nozzles perpendicular to the normal axis of brain surface. The results provided a good, safe, non-thermal effect on the tissue. If the distance of the nozzle did not exceed 30mm, the jet stream’s diameter was approximately 0.3mm². Sharp dissection of biological tissue was possible. It spared the structures of higher solidity (blood vessels). Vessels larger than 20 μ m were preserved after a water jet stream cut. The cuts were deeper in white tissue than in gray tissue. This probably attributed to the higher content of small vessels and dendritic connections horizontal to the brain surface in gray tissue. The best cutting result were obtained by the 0.2mm diameter at 3bar pressure. The cut was precise and shown a fine delineation. The depth of cut from this cutting condition was in suitable range (3.0-4.5mm) and the difference between two types of tissue was only slight (1.5mm). With this condition, water consumption of saline solution was

⁸ Tissue structure or organization

acceptable. Only the smallest diameter showed technical problems of obstructions. The cutting velocity for the efficient cuts could be determined to be between 150–200mm/min, which allowed transaction of tissue in realistic time range. The off-distance between the nozzle and tissue was between 5-10mm in fairly wide range, which allowed cutting without contact to the tissue. The result indicates that the bigger the nozzle diameter, the deeper the cut is. The depth of cut generated by 0.4mm nozzle was twice deeper than the depth generated by the 0.2mm nozzle.

Toth S, et al. (1987). In the surgery of meningiomas⁹, one of the most delicate is separation of the tumor from the brain surface. Water jet was found to be the most effective approach to remove the tumors from the brain surface, cranial nerves, and vessels preserving these structures anatomically and functionally. The jet stream can spread into a performed space. According to the pressure law of fluids the separation pressure is equal or less than the source of fluids without evoking high-pressure spots during the separation. This proved to be the gentlest method among the separation techniques. The water jet is directed into the tumor-arachnoidea space while the free edge of the tumor sheet is gently pulled. As the fluid spreads into the tumor-arachnoidea space, it separates the tumor from the arachnoidea covered brain surface. The remarkable difference from any other water jet surgery is the low working pressure. It is measured between 300-1000 mm of water or 0.03bar –0.1bar. The results obtained from 55 cases of patients were anatomically excellent.

Sohn N, et al. (1977) used the pulsating water jet lavage (Water Pik) in the care of the perineal¹⁰ wound which can be efficiently debrided and cared for by a patient on an ambulatory basis is stressed.

⁹ A slow-growing encapsulated tumor arising from the meninges and often causing damage by pressing upon the brain and adjacent parts.

Kobayashi M, et al. (1995). The Water jet angioplasty¹¹ was studied in vitro, using agar phantom and autopsied aorta, and in vivo in acute and chronic arterial occlusions in mongrel¹². The water jet angioplasty was effective against acute obstructions, but not against chronic obstructions. The results suggest that water jet angioplasty may be effective against arterial obstruction due to acute thrombus¹³

Schurr MO, et al. (1994) compared four types of surgery dissector (electrosurgery (mono and bipolar), thermal lasers and water jet). In parenchymatous 14 tissue the water jet was found to be the least traumatic technique, followed by bipolar high frequency, laser and monopolar high frequency. But water jet was not applicable for intestinal dissection.

Cuschieri A (1994) investigated in water jet cutting. It was considered unsafe for both open and endoscopic surgery undergoing procedures for cancer because of the risk of tumor seeding within the peritoneal cavity. He tried to solve three problems: backspray with fouling of the optic, poor control of the depth of cut and detachment of tissue fragments and isolated cells, which contaminate the operative field.

Harvey RL, et al. (1996) reported the literature review and the case of a limb-threatening injury to the lower extremity caused by water jet stream.

Ray SA, et al. (1992) reported a case of severe full caused by high-pressure washer machine. A 62-year-old male was admitted to the surgical department with an infected burn of right foot. Four days previously he had been using a steam hose to clean his lorry when the jet accidentally swept across his right shoe which already had a small

¹⁰ The area between the anus and the posterior part of the external genitalia

¹¹ Surgical repair of a blood vessel; especially : BALLOON ANGIOPLASTY

¹² An individual resulting from the interbreeding of diverse breeds or strains

¹³ A clot of blood formed within a blood vessel and remaining attached to its place of origin

hole on the dorsum. He was noted to have a 3cm. X 3cm. Blister on the dorsum. High-pressure industrial washers can deliver water stream at 150bar and 140°C at the rate of 15 liters/min—they may therefore conduct up to 25,000 calories per second of heat energy to an area of skin. It is already know that a full skin thickness burn will result from exposure of skin to water at 60°C for 1 minute or 85°C for 10 seconds. Any burns resulting from their use should be treated with caution and full skin thickness damage ruled out before the patient is discharged.

Alitavoli M; Mcgeeeough J.A. (1998) used water jet to conducted experiments on cutting soft materials such as food and meat (pork and beef chicken and lamb were used). Various operations within the water jet cutting process in relation to these specified meat end products were investigated. The tests revealed that water jet may be successfully applied to beef and pig meat, al tough further trials were necessary to explore the potential advantages of this technique to industry, especially for cutting through one. Both pure water and abrasive-added were employed as the cutting medium. In their experiment, sugar was used as the abrasive. The inclusion was found to improve remarkably the bone cutting action. Pressure from 150MPa to 400MPa, nozzle diameter 0.2 to 1mm, stand-off distance 20-25mm, and the traverse rate 2.2-7mm/s were used to cut the meat. The results showed an almost linear relation between depth of cut and pressure applied. Number of passes were also affected the depth of cut. In order to cut 5 mm. Deep, 8 passes have to be performed.

¹⁴ The essential and distinctive tissue of an organ or an abnormal growth as distinguished from its

2.2 Finite Element Analysis of Skin Models

Larabee and Galt (1986) used finite element analysis model represented an animal skin deformation model. Their study was based on two-dimensional geometric models, which ignore the elastic properties of skin and its subcutaneous attachments. The mathematics model used to simulate wound closures such as ellipse and rectangular advancement flaps. In addition, the relationship between the various elastic constants was investigated. The major goal was to design a model for a skin deformation which, if not totally accurate, was an improvement over the current geometric models and was simple enough to be potentially useful as either a training device or as a research tool for design of skin flap surgery. Their models used of only linear isotropic stress and strain range, and the viscoelastic properties were ignored. Young's Modulus, Poisson ratio and spring stiffness constants were the concern parameters. Poisson's ration was kept at 0.5 (which is the ratio of an incompressible solid). The experiments were performed on the piglets to obtain actual deformation grids, which could be correlated with the finite element models. The major variance between the model simulation and the actual experiment was the absolute width of skin strip. They also claimed, in spite of many limitations, the model developed provided a more accurate description of skin deformation during the wound closure than any current techniques.

Kirby, Wang, To, and Lampe (1998) studied and expanded the scope of soft tissue finite element modeling. Three-dimensional model of skin was created as a nonlinear anisotropic material in a laminated-composite structure undergoing large strain and deformations. The model represented local flaps that are frequently used following tumor resection or traumatic tissue loss. The study focused on the deformation of the skin-flaps.

resection or traumatic tissue loss. The study focused on the deformation of the skin-flaps. Hooke's law didn't apply with this nonlinear model. They said that there were a number of authors have purposed strain-energy equations to provide a more rigorous approach than Hooke's law. The idea of their model was adopted from work of Larabee and Galt (1986). The independent variables (Magnitude of subcutaneous adhesion; kN/m and the degree of undermining; Distance:cm) were all so adopted. The dependent variables were the force to closure and the distortion field. The closure ranged from 4.4N to 5.2N and the distortion field ranged from 4.7–5.9cm. As the spring force was increased from 2kN/m to 20kN/m, the distortion field decreased from 5.8 to 4.7cm (-19%), while the closure force increased from 4.5N to 5.2N (+16%). Despite the insensitivity of the relationship, the nonlinear bio-mechanical approach was a valuable development.

2.3 Limitations

The studies reviewed are obviously seen that there was a limitation to obtain accurate skin properties for water jet cutting because there is always a range of values in each property. Human skin properties individually vary from sites, ages, sex, and environments. Besides the difficulty in measuring in vivo skins always caused those authors to make a reasonable assumptions according to the concerning properties. The following are some observations that have been made.

1. There are few researches, published in the literature dealing with finite element analysis of soft tissue especially in finite element analysis of skin.
2. The mechanical properties of different layers of skin are very limited according to the environmental conditions and all the material data are not

available. Most authors did not consider skin as layers. They used just only an average value to represent a whole skin model.

3. There is no information on how the skin will be affected under different pressures of water jet and what is the minimal pressure that will cause the shear of the skin. The papers reviewed also show that water jet is used to do the surgery. They are used to remove tumors, blood clots with special kind of equipment. But the cutting parameters were very different in magnitude.

CHAPTER 3

OBJECTIVES AND PROCEDURES

As shown from the literature review of previous studies, many researches focused on preserving blood vessels, nerves, or minimal bleeding of cut tissues and used a wide variety of cutting parameters such as pressure, nozzle diameters, stand-off distance, even on the same type of tissue. Therefore, the main objective is to find out that what pressure of water jet will make a cut on the layer and also to study the behavior of the skin layers at increasing pressures.

The proposed approach is to carry out a computational study using finite element method to observe and determine the effects of the water jet pressure on the skin. Since the skin is a composite material consisting of various layers and bio-materials, each having individual mechanical properties therefore to study the effect on each layer, it is necessary to obtain the complete set of data. The procedures to fulfill the required objective are as follow:

1. To obtain the available data about the mechanical properties and structure of human skin in order to create a model.
2. To create an effective finite element of skin model using I-DEAS.
3. To get a good representative model of human skin and defining all the material properties of different constituents of the skin layers.
4. To conduct nonlinear static analysis of the model under different sets of operating parameters.
5. To evaluate the effective pressure on the layer of the skin in order for shear to happen.
6. To interpolate the relationship between different performance parameters.

CHAPTER 4

FRAME WORK OF WATER JET CUTTING OF SKIN

In order to operate water jet cutting machine, there are some significant parameters to be concerned with i.e., cutting parameters, structures of skin, mechanical properties of skin, finite element models, and governing equations of the analysis. All of these factors have to be taken in account so that the reliable analysis result would be obtained.

4.1 Water Jet and Its Operating Parameters

The cutting capabilities of water jet depends on a number of factors including the type of materials, the composition of the working fluid, the method of machining, and the direction of the liquid jet with respect to the material surface. Low-strength materials are easier to cut. They require a lower jet pressure. For instance, jet pressure at 200MPa is used to cut plywood, leather, or rubber. At 200-500MPa can be used to cut plastics. At 500-700MPa and 700-1000MPa are used to cut light metals and steel [Tikhomirov RA, et al.]. The pressure that is used for surgical tool is significantly lower than industrial uses. It varies from 0.003MPa to 40MPa but there is an exception on HydroBlade keratomes that uses a high-energy beam of water (diameter 0.03mm) at 1360bar (approx. 136MPa) Gordon E, et al. (1998) to cut a flap in cadaver eye.

Cutting agent (working fluid) also has a great effect on the jet compactness, and cutting capability. A small ratio of additive that added to the working fluid can improve the productivity of sheet cutting up to 35% [Tikhomirov RA, et al.]. Soluble polymers that added will reduce the dispersion of the jet profile and keep the width of jet stream effective along within the stand-off distance.

4.1.1 Operating Parameters

Water jet systems consist of many components and many variables. In order to control the cutting parameter effectively, these parameters have to be taken in account to obtain the good cutting results. Water jet machines physically have many important components such as hydraulic intensifier, Pressure reservoir, and nozzle. These components determine the characteristics of the machines, which can be categorized into four groups.

Table 4-1 Cutting parameters of water jet.

Pressure Intensifier	Nozzle	Work piece characteristics	Process characteristics
-Intensifier Efficiency	-Nozzle Diameter	-Material Properties	-Depth of Cut
-Horse Power	-Nozzle Structure	-Material Thickness	-Width of Cut
-Pressure Ratio			-Stand-off Distance
-Flow Rate			-Exposure time

To explain the how each parameter can control the cutting characteristics. The illustration will be used to describe the cutting processes.

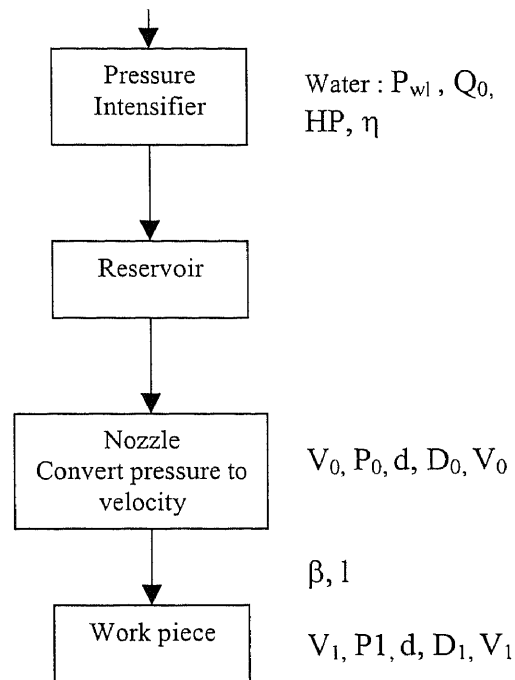


Figure 4-1 Cutting parameters and its components.

$$Q_0 = \frac{HP \times \eta}{P_{wl}}$$

Assume that there is no loss, $\eta = 1$

Q_0 = Flow rate of water

HP = Power of the pressure intensifier (Horse Power)

η = Efficiency constant of the intensifier

P_{wl} = Pressure of water that produced by intensifier

$$V_0 = \frac{Q_0}{A_0} = \frac{Q_0}{P_1 d^2}$$

$$D_1 = D_0 \varepsilon^{-\beta l}$$

where β is the flare angle constant (0.030 and 0.015) and

$$V_1 = V_0 e^{-\beta l}$$

V_0 = Velocity of jet stream at the end of the nozzle

V_1 = Velocity of jet stream at the surface of the work piece (skin)

P_0 = Pressure of water at the end of nozzle

d = Diameter of the nozzle entrance

D_1 = Diameter of the jet stream at the surface of the work piece

D_0 = Diameter of the jet stream at the end of the nozzle

β = Fare angle constant

l = Stand-off distance between the tip of the nozzle and the surface of work piece

Assume that there is no energy loss between nozzle and work piece. Kinetics energy will be equal between the orifice and the surface of the work piece.

$$K.E._0 = K.E._1$$

So the pressure of the jet stream is obtained at the surface of the work piece

$K.E._0$ = Efficiency constant of the intensifier

$K.E._1$ = Efficiency constant of the intensifier

$$Q_0 P_0 = Q_1 P_1$$

$$P_1 = \frac{Q_0 P_0}{Q_1} = \frac{Q_0 P_0}{V_0 A_0}$$

4.2 Structure and Mechanical Properties of Skin

Skin of human is a large organ comprising a sheet like investment of the whole body, which adapts admirably to its contours and neatly conforms to the movements of the organism within. Skin of the average adult human exceeds 2m^2 in area and is in most places no more than 2mm in thickness. Two major tissue layers are conventionally recognized as constituting human skin. The outer layer is a thin stratified epithelium, the epidermis, which varies relatively little in thickness over most of the body, between 0.075mm to 0.150mm, except on the palms and soles where the thickness may be 0.4-0.6mm. underlying the epidermis is a dense fibroelastic connective tissue called the dermis, which constitutes the mass of the skin. There is considerable variation in the thickness of the dermis in different regions of the body [Rushmer et al., 1966]. The dermis supports extensive vascular and nerves networks and encloses as well specialized excretory and secretory glands and keratinized appendage structures, such as hair and nail. Besides it contains collagen, elastin, reticulin, fibrocytes, blood and lymph vessels. All are embedded in what is called the ground substance—a gelatinous matrix consisting of water, mucopolysaccharides, protein (mostly soluble collagen) enzymes, and electrolytes. Beneath the dermis is the subcutaneous tissue, or hypodermis, which is variably composed of loose areolar connective tissue or fatty connective tissue displaying substantial regional variations in thickness. Fibrous band, continuous with the fibrous structures of the dermis, penetrate and thereby lobulate the subcutaneous tissue and form attachments of the skin to underlying fibrous skeletal components such as fascial sheets. Substantial regional variability in the appearance and texture of the skin results from the regional variation blood flow, but more particularly from the distribution of glandular structures and varying of hairiness.

4.2.1 Skin Components and Mechanical Roles

The predominant components for 60 to 80 percent of the dry weight of skin depending on age, sex, and site. The collagen appears as a three-dimensional, apparently disordered, network of wavy or coiled fibers. They are structured in several layers of preliminary planar networks, with some fibers running between them. Collagen fibers near the epidermis are finer and randomly oriented [Skalak R, et al], while at the mid-zone they are coarser and densely packed, and maybe show preferred orientation. In the deep zone they are coarse but loosely packed.

The ground substance matrix accounts for 70-90 % of skin's volume. Although it was traditionally considered to be amorphous, there is evidence, which suggests that some components of the ground are incorporated in the structure of the collagen fiber [Skalak R, et al].

Collagen fibers are the major mechanical elements in the skin. When these fibers are stretched, their effects predominate over those of all components. They are strong and stiff. Thermodynamic studies have revealed that collagen behaves like a crystalline rather than a rubber-like material. In response to uniaxial stretch the skin contracts in the lateral direction and the collagen fibers gradually align themselves in the direction of stretch. Their packing becomes denser and they subsequently stretch [Skalak R, et al]. The fibers' alignment increases strength and stiffness in the direction of the stretch—an important merit in the tissue, which may be stretched in various directions. From the study of Park and Lakes (1992) found that the Young's modulus of collagen is 1GPa and the tensile strength is 50-100MPa.

Elastin accounts for about 4% of the dry weight. It is considerably less stiff than

collagen. Its elastic properties are related to configuration entropic changes as in rubber and rubber like materials. It is appears as fine fibers, which intertwine around the thicker collagen fibers in the deep layers of the dermis, but are rather straight close to the epidermis [Skalak R, et al]. Young's modulus of elastin is 0.6MPa and the tensile strength is 1MPa.

Reticulin fibers accounts for 0.4% of the dry weight of the skin [Skalak R, et al]. They are located around blood vessels and hair, close to epidermis. Their chemical composition is similar to that of collagen. Because of their minute quantity, They have very little effect on the skin's overall response.

The overall tensile strength of skin has typical value in the range of 2.5MPa to 16MPa [Skalak R, et al]. It varies with site [Richard et al.], it higher in the main fiber direction, is higher in males than females [Richard et al.] and is believed to increase with age. Skin may also break under considerably lower stresses (as low as one-fifth of the tensile strength under long creep test [Richard et al.]).

The Young's modulus of epidermis has a range of 1 to 10GPa (@ 25-30% relative humidity). It is significantly influenced by both humidity and temperature [Richard et al.] but at 100% humidity the Young's modulus has two to three linear regions with and initial slope which is 1000-fold smaller than in dry state [Richard et al.] The tensile strength of epidermis varies from 10–100MPa.

The Young's modulus of dermis is 100MPa and the tensile strength is 5MPa. For subcutaneous layer, it has the Young's modulus of 50MPa and the tensile strength of 5MPa, which is found in Arif (1997).

CHAPTER 5

PROPOSED METHODOLOGY

5.1 Finite Element Analysis Method

Finite Element Analysis (FEA) is a process, which can be used to solve engineering problems such as deflection and stress on a structure, heat transfer, fluid flow, or electrical fields, etc. Finite Element Modeling (FEM) divides the structure into a grid of “elements” which form a model of the real structure. Each of the elements is a simple shape (such as a square or a triangle) for which the finite element program has information to write the governing equations in the form of a stiffness matrix. The unknowns for each element are the displacements at the “node” points, which are the points at which the elements are connected. The finite element program will assemble the stiffness matrices for these simple elements together to form the global stiffness matrix for the entire model. This stiffness matrix is solved for the unknown displacements, given the known forces and boundary conditions. From the displacements at the nodes, the stresses in each element can then be calculated. A finite element is derived by assuming a form of the equation for the internal strains. Some elements are defined to assume that the strain is a constant throughout the element, while others use higher-order functions. Using these equations and the actual geometry of a given element, the equilibrium equations between the external forces and the nodal displacements can be written. There will be one equation for each degree of freedom for each node of the element. These equations are most conveniently written in matrix form for use in a computer algorithm. The matrix of the coefficients becomes a “stiffness matrix” that relates forces to displacements.

$$\{F\}=[K]*\{d\}$$

Even though the unknowns are at discrete degrees of freedom, the internal equations were written for strain functions that represent a continuum. This means that even though the finite element model has a discrete number of equations, if the right elements are chosen, it is possible to converge on the correct answer with a less-than-infinite number of nodes and elements. A finite element model is the complete idealization of the entire structural problem, including the node locations, the elements, physical and material properties, loads and boundary conditions. The model will be defined differently for different types of analysis: static structural loads, dynamics, or thermal analysis.

The accuracy of the resulting solution will depend on how well the structure was modeled, the assumptions made for loads and boundary conditions, and the accuracy of the elements used for the given problem. In general, the solution will be more accurate as the model is subdivided into smaller elements. The only sure way to know if the model has sufficiently converged on the final solution is to make more models with finer grids of elements and check the convergence of the solution.

5.1.1 Linear Static Analysis

In linear analysis, the displacements of the finite element assemblage are infinitesimally small and that the material is linearly elastic. In addition, the nature of the boundary conditions remains unchanged during the application of the loads on the finite element assemblage. With these assumptions, the finite element equilibrium equations derived were for static analysis.

$$KU = R$$

This equations correspond to a *linear analysis* of a structural problem because the displacement response U is a linear function of the applied load vector R . For example, if the loads are αR instead of R , where α is a constant, the corresponding displacements are αU . When this is not the case, we perform a *nonlinear analysis*. The linearity of a response prediction rests on the assumptions just stated, and it is instructive to identify in detail where these assumptions have entered the equilibrium equations above. The fact that the displacements must be small has entered into the evaluation of the matrix K and load vector R because all integration have been performed over the original volume of the finite elements, and the strain-displacement matrix B of each element was assumed to be constant and independent of the element displacements. The assumption of a linear elastic material is implied in the use of a constant stress-strain matrix C , and, finally, the assumption that the boundary conditions remain unchanged is reflected in the use of constant constraint relations for the complete response. If during loading a displacement boundary condition should change, e.g., a degree of freedom that was free becomes restrained at a certain load level; the response is linear only prior to the change in boundary condition. This situation arises, for example, in the analysis of a contact.

5.1.2 Nonlinear Static

Essentially, all Static structure analysis problems are to some degree nonlinear. Whenever loads, material properties, contact conditions, or structural stiffnesses are a function of displacement, the problem is nonlinear, If large displacements or rotations are present, the linear strain-displacement relations assumed in linear analysis may also be

inadequate. The Nonlinear Static Analysis is a structural finite element solver that takes into account of geometric and material nonlinear behavior. It is capable of performing the following types of analysis:

- Geometric nonlinear analysis – large displacements and rotations including arc-length method for buckling and post-buckling

- Material nonlinear analysis – plasticity or creep

- Combined geometric and material nonlinear analysis

Compared to a linear analysis, significantly greater computer time and disk storage is required for a nonlinear analysis.

Nonlinear Static Analysis solves for the displacements, strains, stresses, etc. of the finite element model at these discrete time intervals in the history of the structure. The manner in which time is used in the analysis depends on the material model selected. For linear material or a material nonlinear analysis with plasticity, time is a convenient way of in putting load histories, but otherwise plays no part in the analysis. If creep is selected, the creep strain rates must be integrated over time. Before using the nonlinear solver for a material nonlinear analysis, the analysis must be prepared by defining plasticity and/or creep options. A nonlinear solution proceeds incrementally with equilibrium iterations performed at every solution point.

Table 5-1 Classification of non-linear analysis and governing equation.

Type of analysis	Description	Typical formulation used	Stress and strain measures
Materially-nonlinear-only	Infinitesimal displacements and strains; the stress-strain relation is non-linear	Materially-nonlinear-only (MNO)	Engineering Stress and strain
Large displacement, large rotations, but small strain	Displacements and rotations of fibers are large, but fiber extensions and angle changes between fibers are small; all the stress-strain relation may be linear or nonlinear	Total Lagrangian (TL)	Second Piola-Kirchhoff stress, Green-Lagrange strain
		Updated Lagrangian (UL)	Cauchy stress, Almansi strain
Large displacement, large rotations, but large strain	Fiber extensions and angle change between fibers are large, fiber displacements and relations may also be large; the stress-strain relation may be linear or nonlinear	Total Lagrangian (TL)	Second Piola-Kirchhoff stress, Green-Lagrange strain
		Updated Lagrangian (UL)	Cauchy stress, Logarithmic strain

Source: Finite Element Procedure. Klaus-Jurgen Blathe (New York: McGraw-Hill, 1996) 448.

The table above shows a classification that is used conveniently because it considers separately material nonlinear effects and kinematics nonlinear effects. The most general analysis case is the one in which the material is subjected to large displacements and large strains. In this case the stress-strain relation is also usually nonlinear.

Nonlinear Static Analysis uses an Updated Lagrangian formulation for geometric nonlinear and combined geometric and material nonlinear analysis. With this formulation the finite element equilibrium equations are written with respect to the current configuration of the structure.

The finite element equilibrium equations may be derived in different ways, but the most common technique for the displacement-based finite element method uses the principle of virtual work. The principle of virtual work states that:

A loaded deformable body is in equilibrium if the total virtual work of the real external forces and moments is equal to the virtual work of the real internal stresses when subjected to any virtual displacements consistent with the

For a linear formulation, the integrals in the equilibrium equation are computed over the initial configuration of the body. Strain is a linear function of displacement, $\{\varepsilon\} = [B] \{u\}$, and is linearly decomposed into elastic and thermal components:

$$\{\varepsilon\} = \{\varepsilon_E\} + \{\varepsilon_T\}$$

Stress is a linear function of elastic strain:

$$\{\sigma\} = [D] \{\varepsilon_E\}$$

where $[D]$ is the temperature dependent matrix of elastic constants. The linear equilibrium equation is then written in the familiar form:

$$[K]\{u\} = \{F_I\} + \{F_S\} + \{F_B\} - \{F_T\}$$

where $[K]$ is the linear stiffness matrix which is computed from:

$$[K] = \sum_{\text{elem}} [k] = \sum_{\text{elem}} \int_{V_e} [B]^T [D] [B] dV_e$$

The global force vectors due to surface tractions, body forces, and thermal strains are respectively:

$$\begin{aligned}\{F_s\} &= \sum_{\text{elem}} \int_{S_e} [N]^T \{f_s\} dS_e \\ \{F_B\} &= \sum_{\text{elem}} \int_{V_e} [N]^T \{f_B\} dV_e \\ \{F_T\} &= \sum_{\text{elem}} - \int_{V_e} [B]^T [D] \{\varepsilon_T\} dV_e\end{aligned}$$

Some of the force terms in the equilibrium equation may be a function of displacement, or stress may be a nonlinear function of strain as a result of material nonlinearities such as plasticity or creep. In such cases, a nonlinear solution may be required.

The equilibrium equation can be restated in the form of a residual force that is a measure of how much the solution deviates from equilibrium. The residual or out-of-balance force is given by:

The solution of the equilibrium equation is iterative and thus will successively generate improved estimates of the solution. The iteration is terminated when the specified convergence criteria are satisfied, when the number of specified iterations is exceeded, or when the solution diverges.

The stiffness matrix in the nonlinear solution does not participate in the equilibrium statement as is the case in linear analysis. The stiffness simply relates incremental displacements to incremental forces. The tangent stiffness at a particular time will depend on temperature, geometry, material nonlinearities, and stress stiffening effects. If the tangent stiffness is updated every iteration, the procedure is called a full Newton-Raphson method. If the stiffness is only periodically or never updated, the

procedure is called a modified Newton-Raphson procedure. A general discussion of these techniques may be found in Bathe (1996).

A nonlinear solution may not always converge or may not converge to the desired accuracy within the specified number of iterations. If this situation occurs, you may need to subdivide the loading into more steps, select a more conservative procedure for reforming the tangent stiffness and/or modify the number of iterations allowed. You can then restart the solution from a previously converged equilibrium solution.

5.2 I-DEAS (Finite Element Analysis Module)

I-DEASTM (Integrated Design Engineering Analysis Software), a Unix workstation-based application, is an integrated package of mechanical engineering software tools. This software was designed to facilitate a concurrent engineering approach to mechanical engineering product design and analysis. The wide variety of the software allows users to be able to develop and modify the ideas in the same time. It is composed of a number of software modules called “application”, each subdivided further into “tasks”, all executed from a common menu and sharing a common database.

5.3 Modules of Modeling/Analysis

5.3.1 Geometric Modeling

Geometric modeling is the module that can generate two-dimensional or three-dimensional solid part model geometry of work pieces. In I-DEAS, the geometric module is called “Master Modeler”. The master solid model is the starting point and a shared information source containing the geometric definition of the parts and assemblies in the

concurrent engineering design project. The solid model can be used for many “downstream” uses such as interference studies, mass properties calculation, kinematic analysis, stress analysis, dynamic analysis, manufacturing, testing, or the other applications. This module facilitates this information sharing by storing part models in the central library.

5.3.2 Meshing Module

Meshing module is an application in I-DEAS Simulation application that used to perform finite element simulation. The most common solution type is linear static to calculate deflections and stresses. The part geometry is subdivided into a mesh of elements, which are used to calculate the stiffness of the structure and solve for deflections, given the loads and boundary conditions.

As we know, every element needs nodes to be the connections between other element surround them. So node creation has to be done prior to create elements on the geometry models. Nodes can be created manually by keying in their coordinates or generated by copying, reflecting, or generating nodes between two other sets of nodes. Nodes are created by specifying the coordinates in any existing coordinate system. This is called the “definition” coordinate system for the node. Nodes also have another coordinate system called the “displacement” coordinate system. A displacement coordinate system other than the global cartesian system can be used by modifying the nodes after those element have been created. This can be used to supply a boundary condition in a cylindrical coordinate system, for example. Three kinds of coordinate systems are available in I-DEAS Simulation: cartesian, cylindrical, or spherical. These three coordinate systems are pre-defined. Other local coordinate systems can be added to

the model by translating or rotating one of these types. Coordinate systems can be created and then translated and rotated, or created by defining them with respect to an existing coordinate system. When meshing on a part, the coordinate system of the part is used. This will usually be aligned with the global coordinate system, but not always.

Elements can be manually created by picking nodes or by generating elements from existing elements. But they can also be generated automatically. Elements can be created by copying or reflecting, like nodes. These operations will create nodes and elements at the same time. These copy and reflect operations create elements of the same type as the parent elements set. Other types of element generation such as “extrude” or “revolve” create elements of a different type. For example, “extrude” quadrilateral elements into 8-noded solid elements. This is a useful method to generate 8-noded solid brick elements without using mapped mesh volumes. A similar element generation method can create thin shells on the surface of solid elements by using the “surface coating” creation command. Elements contain an element label, an element type, a list of nodes that make up the element, a color, a material property table ID, and a physical table ID. Any of these element attributes can be modified after the element is created, but the element type can’t be modified to a type that uses a different number of nodes.

There are two types of meshing. The first type is mapped meshing. Mapped mesh is a regular mesh on surfaces or volumes. A surface uses 2D shell elements, while a volume uses 3D solid elements. Mapped meshing cannot be used on curves or edges. Mapped meshing requires that a surface has three or four sides. A three-sided surface must have an equal number of elements on any two of the opposite sides. A four-sided surface must have an equal number of elements on one pair of opposite sides, but may

have an equal or unequal number on the other pair of opposite sides. A surface cannot have holes. Likewise, mapped meshing requires that a volume has five or six sides. The volume cannot have holes, and opposite sides of the volume must have an equal number of elements defined. Unlike surfaces, volumes must have equal numbers of elements on opposite sides.

Free meshing, second method of meshing, generates (2D) triangular or rectangular elements on target surfaces and generates (3D) tetrahedron or wedge elements on target solid. This type of meshing cannot be created manually. But it has no limitation on the shapes of target model. The size of elements is control by the global minimum size. The smaller the global minimum size is, the bigger number of elements on the model is.

5.3.3 Model Verification

The Meshing task also contains several checks to verify any identify modeling errors in finite element models. Typical problems that can be verified are duplicate nodes, duplicate or missing elements, and highly distorted or warped elements. One of these verifications is an element free edge verification. This verification will plot the free edges of elements not connected to another element. This can be a very useful verification in finding element connectivity problems. Normally, this will plot the outer boundary of the model, which is where the elements are not connected to others. If elements adjoin each other edge to edge but reference duplicate coincident nodes rather than share the same nodes, an extra line will show up in the free edge plot. This represents a “crack” in the

model. Duplicate elements defined by the same nodes will cause neither element to be plotted in this verification, and a missing line may show up in the plot.

Element distortion is another popular verification. Values are reported by the distortion check from -1.0 to 1.0 . A value of 1.0 represents a perfect square (a circle fits inside). Values less than 0.0 are horrible. A typical rule of thumb is that values should be between $.4$ and 1.0 but there is no exact cut-off for what is not acceptable. It depends on the type of analysis to be performed and where the badly distorted elements are located in the model. Avoid highly-distorted elements in important areas such as high stress locations. Sometimes, due to the geometry you are modeling, distorted elements can't be avoided. Other element quality checks include checks for warping out of plane, interior angles, mid-side node placement, and coincident elements. There is a coincident node verification to detect coincident nodes within a small tolerance supplied by the user. This command will optionally renumber adjacent elements so that they share the same nodes. This is called "merging" out the duplicate nodes.

5.3.4 Analysis Module

In I-DEAS, the analysis module is called Model Solution Task. Model Solution Task in the Simulation application is where the finite element model is solved. There are several types of analysis can be performed such as static, buckling, heat transfer, potential flow, dynamics, and non-linear. To use this module the finite element model must be created in the model file as well as boundary condition and forces must also be created and selected in to boundary condition sets.

5.3.5 Post Processing

The Post processing task of the Simulation application provides tools to display and interpret the results after the analysis is finished and the result is obtained. The results can be brought in from external finite element analysis programs for post-processing. Several different display types are available including contour plot and deformed geometry plots.

Calculations result to be displayed are stored in “Data sets” or “Groups”

Displacements will be stored in one data set, and stresses in another. The other data sets can be stored as well, depending on requested for output selections in the Solution Set, such as element forces, reaction forces, and strain energy. Components of both stress and deformation can be displayed in the same time but other than these two the display will show the results superimposed on the deformed model.

5.4 Design of Experiments

In order to know the behavior of skin model, numbers of experiments have to be conducted. The experiments are designed to reflect how each parameter will effect the results. The water jet cutting has many factors, Some factors are very important and needed to be the input parameters of the finite element analysis. Finite element analysis requires a set of forces or pressures that can cause the stress or strain on the work piece. But the forces or pressures are not the nominal force or pressure indicated on the water jet machine. They have to be the actual forces or pressures apply on the finite element models, which can be derived from the calculation using other parameters of the water jet it self such as orifice diameter, pressure in the reservoir, flow rate, stand-off distance,

flare angle constant, pump power, pump efficiency, etc. For these experiments, the independent variables of the analysis are the cutting pressures (pressure that applied on the surface of the skin), the nozzles diameters, the stand-off distances, and the flare angle constants. The ranges of these factors are set up based on the values founded in the literature review.

According to the governing equations and assumption the mentioned before in chapter 4, Start from a 3000Watts motor of the pump, and assume that there is no power loss in the process (pump efficiency equals 1.0) and the flare angle constants of 0.015 and 0.03 are selected. 5mm and 10mm are the selected values of the stand-off distances. The four values of pressure of water in the reservoir are selected from 10MPa, 40Mpa, 70Mpa, and 100MPa. There are also three sizes of nozzles are used. —0.1mm, 0.2mm and 0.3mm. All of these are the variables of the experiments. The table below shows the independent variables, which will be the input of the analysis. There are 48 analyses based on those independent variables but there are some of analysis that are not required to conducted because all of their input values are identical. They can be analyzed together at the same time. For example, Solution number 2 and 3 have same value of pressure and effective diameter. Thus there are only 36 analyses are needed to be analyzed.

5.5 Curve Fitting (Parameter Estimate)

The results obtained from the finite element analysis are the sets of the maximum shear stress for nodes. In order to interpret the set of the raw data to a meaningful result. Curve fitting is the method that takes the values of the points into the mathematics equations and finds the ideal equation to describe two-dimensional empirical data. This equation will reflect the nature of the data set and has capability in predicting the values. TableCurve is the software that provides the curve fitting in this thesis. Once the fit is complete, TableCurve presents it with a statistically ranked list of the best fit equations, to select the best fit equation, The R^2 of that equation should be maximal, which means less errors are found and more accurate the equation.

CHAPTER 6

CASE STUDY

6.1 Assumptions

Skin properties are highly variable depending on species, age, exposure, hydration, obesity, and biological difference between individuals. In the same individuals, skin's properties vary with site and orientation and maybe altered by irradiation, drugs, and chemicals. Besides the difficulty of comparing in vivo and in vitro responses of the same specimen both because of the physiological differences between in vivo and in vitro condition always makes a range of value for each property.

Skin is obviously not a homogeneous material because of the fibrous, cellular, vascular, granular, and amorphous components of which it contains. In particular problems, skin is usually considered in only dimensions of specimens which are orders of magnitude larger than any of skin's components.

6.2 FEA Modeling of Skin

There are three main steps in creating the finite element model of skin. First, the pie-shaped geometry that represents each layer of the skin have to be created in Master Modeler module. Second, apply the boundary condition and pressure to the model then create the finite element model.

6.2.1 Geometric Modeling

The procedures of creating geometric model of the skin are as follow:

Create three pie-shaped under Simulation Application with Master Modeler task.

Set up the unit of the model to millimeter-Newton, which use the unit of length is millimeter and the unit of force is milli Newton. Each pie-shaped represents each layer of skin. The pie-shaped has been selected because it has better stress distribution all over model than using a cube-liked model. Because of the symmetry of the model, only one quadrant of full circle was created. The radius of each layer is 3.0 mm and the thickness is 0.1 mm for the epidermis, 1.6 mm for the dermis, and 0.3 mm for the subcutaneous.

After named all parts, change the application to Master Assembly to assemble those three pie-shaped models into one stack of the skin model. Stacking the part by translating the models until there are 0.01mm gaps between the layer. These gaps represent the bonding between each two layers.

Because there are three different diameters of nozzles, which generate different values of pressure. So three models of skins are created. The only thing that different is the Effective diameter (D_1). The first model that will be applied with 0.1mm diameter has 0.09999mm effective diameter. The second model that will be applied with 0.2mm diameter has a 0.19999mm effective diameter. And the last one that will be applied with 0.3mm has 0.29999mm effective diameter.

6.2.2 Boundary Conditions and Loading

To use symmetry, and the correct restraints along the plane of symmetry where the model is cut, nodes cannot move perpendicular to the plane or rotate in the plane. For example, if the symmetry plane is the plane where X is a constant, all nodes on this plane must be restrained in X translation, Y rotation, and Z rotation. In this model, because of a quadrant of pie-shaped, There are two side surface that comply the symmetry rule above.

The orientation of this model is slightly different from conventional finite element models. The height of this model is aligned to Y axis. There are four different sets of boundary condition were made.

1. The bottom surface is restrained to ground with no translation in any axis. All rotational for each axis is free.
2. The first side surface (the surface that has normal vector aligns to X axis) was restrained with no translation in X axis and no rotational in Z axis. The rest DOF's are free.
3. The second side surface (the surface that has normal vector aligns to Z axis) is restrained with no translation in Z axis and no rotational in X axis. The rest DOF's are free.
4. The back surface (the circumference surface) is restrained with no translation in X, Y and Z and free rotational for all axes.

6.2.3 Element Modeling

Creating a Mapped Mesh on the skin model. Before define mapped meshes for a volume, the model might need to be simplified the shape by dividing it into smaller volumes. Partitioning is the way to divide a complex volume into smaller volumes that can be mapped meshed more easily. And also allow the faces of the partitioned volumes to be applied by pressures, forces, or restraints. In this skin model, the diameter of water jet stream is one of the independent variables. There fore the impact area that the jet approaches should be available to select in order to apply the pressure on the skin model.

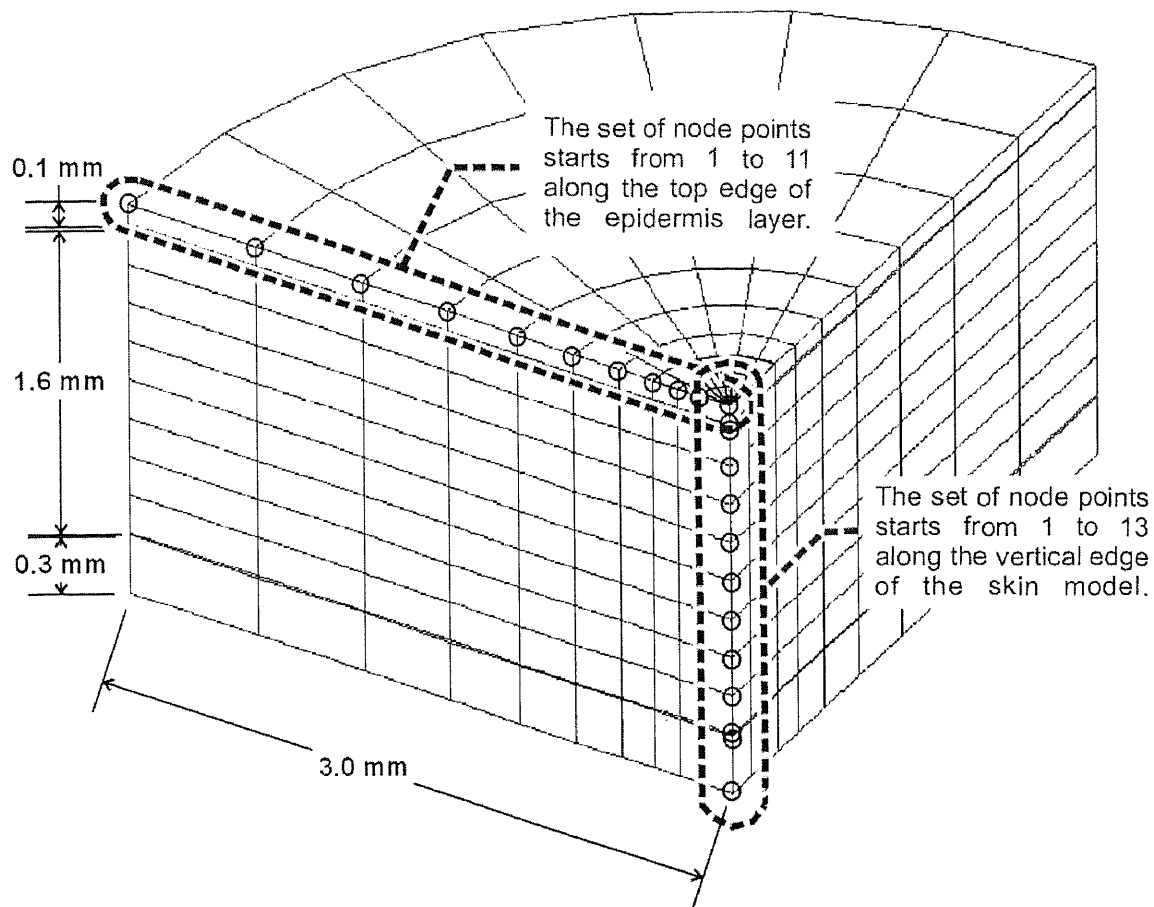


Figure 6-1 The picture of the skin model consists of three layers: Epidermis, Dermis, and Subcutaneous, and two contact sets (Friction gap) between each two layers. It also shows the two sets of node points that are the data sets contain the results

After completing any partitioning, mapped meshing developed on a volume by doing the following:

1. Pick the volumes that belong to epidermis layer, then enter meshing parameters on the Define Mesh form. Pick *Mapped* as the mesh type, and then pick *Mapped Options* to define other parameters.
2. Select the material property for these volumes.
3. On the Mapped Meshing Options form:

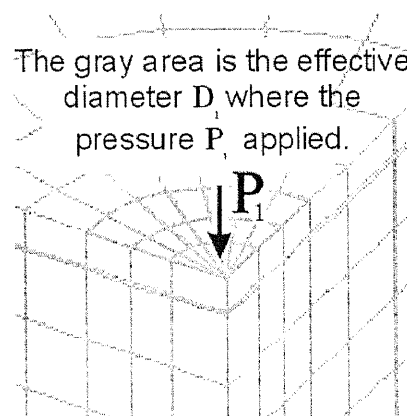
Pick *Define Corners* to identify the three or four corners of the mapped mesh volumes. For a three-corner mesh, it needs to identify the degenerate corners. In the skin model, the centers of each pie-shaped volume should be picked. The surfaces underlying a mapped mesh volume must have three or four “sides”. Each side of the surface being meshed can be a composite of several edges. If any surface has more than three or four edges, *Define Corners* on the Mapped Meshing Options form can be used to define sides for the surfaces.

Pick *Define Elements/Side* to specify the number of elements on each side. When picking *Define Elements/Side* for a volume, the software prompts to enter the number of elements for the sides of the volume. The opposite sides of the volume will automatically be given the same values. (Unlike surfaces, for volumes the software doesn’t allow to have unequal numbers of elements on opposite sides.)

Pick the bias option. This option will make finer mesh in the area that we interested (area that forces or pressure applied). For example, if the number of bias is 6, the longest element on that side will be 6 times longer than the shortest element on that side. The table below shows the value of bias number and number of elements for each side.

Table 6-1 The numbers of Elements and Bias numbers along each side

	Epidermis	Dermis	Subcutaneous
Number of element along the thickness	1	8	1
Number of element along the radius of pie-shaped	10	10	10
Number of element along the Circumference side	7	7	7
Bias number along the thickness	Non-bias	Non-bias	Non-bias
Bias number along the radius of pie-shaped	6	6	6
Bias number along the Circumference side	Non-bias	Non-bias	Non-bias

**Figure 6-2** The picture of the effective radius

Pick (Generate) Solid Mesh. Pick the volume to be meshed. Then the software will generate the nodes and elements under the defined mesh definitions.

Create the beam elements that represent Collagen fibers. Using the Other Type Elements Creating icon and select Beam elements, node connection. Define the element definition and material properties. Select connectivities randomly between two nodes to create a beam elements. 24 beam elements are added to the model on Dermis a subcutaneous layers.

Table 6-2 Element type and meshing method created on the each layer

Skin Layers	Element Type	Meshing Method
Epidermis	Hexahedral	Mapped Meshing
Dermis	Hexahedral	Mapped Meshing
Subcutaneous	Hexahedral	Mapped Meshing
Collagen Fiber	Beam	Node Connection
Contact set	Gap	Contact set

6.3 Element and Material Properties

All of the materials are defined as isotropic materials.

Table 6-3 Mechanical properties of the skin layers including the gap element

Skin Layers	Mass Density (Kg/m ³)	Young's Modulus (MPa)	Poisson's Ratio	Thickness (mm)
Epidermis	1056	1000	0.12	0.1
Dermis	N/A	100	0.12	1.6
Subcutaneous	N/A	50	0.12	0.3
Collagen Fiber	1410	1000	0.12	
Contact set				0.01

6.4 Results

Table 6-4 Extended radius of cut and depth of cut of analyses number 1 to 48

Analysis Running No.	Extended Radius of Cut (mm)	Depth of Cut(mm)	Analysis Running No.	Extended Radius of Cut (mm)	Depth of Cut(mm)
1	0.00	0.000	25	0.03374	0.12786
3	0.00	0.000	27	0.03374	0.12786
2	0.00	0.000	26	0.03374	0.12786
4	0.00	0.000	28	0.03374	0.12786
5	0.00	0.11262	29	0.32985	0.25214
7	0.00	0.11262	31	0.32985	0.25214
6	0.00	0.11262	30	0.32985	0.25214
8	0.00	0.11262	32	0.32985	0.25214
9	0.00	0.12005	33	0.52609	0.40887
11	0.00	0.12005	35	0.52609	0.40887
10	0.00	0.12005	34	0.52609	0.40887
12	0.00	0.12005	36	0.52609	0.40887
13	0.00	0.1173	37	0.07503	0.14622
15	0.00	0.1173	39	0.07503	0.14622
14	0.00	0.1173	38	0.07503	0.14622
16	0.00	0.1173	40	0.07503	0.14622
17	0.17278	0.19928	41	0.41049	0.31339
19	0.17278	0.19928	43	0.41049	0.31339
18	0.17278	0.19928	42	0.41049	0.31339
20	0.17278	0.19928	44	0.41049	0.31339
21	0.38695	0.26415	45	0.60618	0.57391
22	0.38695	0.26415	47	0.60618	0.57391
23	0.38695	0.26415	46	0.60618	0.57391
24	0.38695	0.26415	48	0.60618	0.57391

The results in the table above are obtained from the maximum shear stress results on two sets of nodes previously mentioned. There were two interpretations made in order to obtain the extended radius of cut and the depth of cut.

1. The extended radius of cut is come from the values of Maximum stress appears on the node along the top edge of epidermis layer. This edge contains 11 node points, which reflect different value of maximum shear stress. According to the ultimate tensile strength of the epidermis that mentioned before equals to 10MPa. Therefore if the nodes that have value of stresses exceed the ultimate tensile stress at 10MPa, the tissue on that

points will shear and be removed from the skin body cause a cavity. The extended radius is the widest radius of this cavity, which is the radius on the epidermis layer.

2. The Depth of cut is interpreted in the same way as the radius of cut but it use the vertical edge that pass along the center axis of the skin model. This edge contains 13 points. The first point starts from the top surface of epidermis and the last point is the bottom most located on the bottom surface of subcutaneous layer. The Ultimate tensile strength of the dermis layer is 5MPa. Thus the nodes that have the stress exceed 5MPa will shear and be removed as well.

Table 6-5 Results based on the sizes of the nozzles

	Analysis No.	Pressure (MPa)	Maximum Stress (MPa)	Maximum Displacement (mm)	Extended Radius of Cut (mm)	Depth (mm)
Nozzle 0.1 mm	4	10	1.92	0.012	0.000	0.000
	16	40	8.00	0.018	0.000	0.117
	28	70	14.07	0.025	0.034	0.128
	40	100	20.17	0.031	0.075	0.146
Nozzle 0.2 mm	8	10	5.92	0.020	0.000	0.113
	20	40	23.21	0.050	0.173	0.199
	32	70	40.24	0.075	0.330	0.252
	44	100	57.31	0.100	0.410	0.313
Nozzle 0.3 mm	12	10	9.66	0.029	0.000	0.120
	24	40	37.72	0.080	0.387	0.264
	36	70	65.97	0.127	0.526	0.409
	48	100	94.18	0.173	0.606	0.574

Relationship between Pressure and Maximum Stress

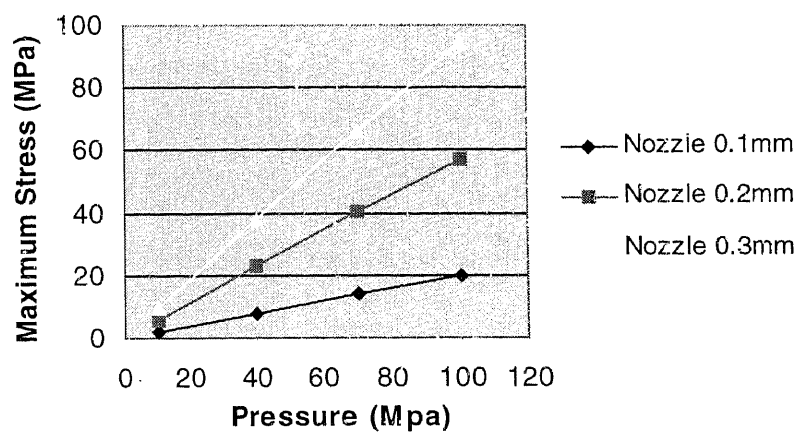


Figure 6-3 The relationship between the pressure and the maximum shear stress based on the nozzle sizes

Relationship between Pressure and Maximum Displacement

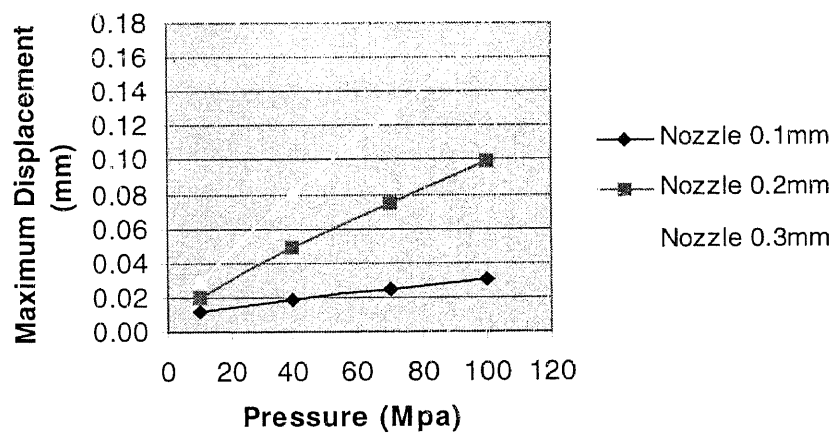


Figure 6-4 The relationship between the pressure and the displacement based on the nozzle sizes

Relationship between Pressure and Extended Radius of Cut

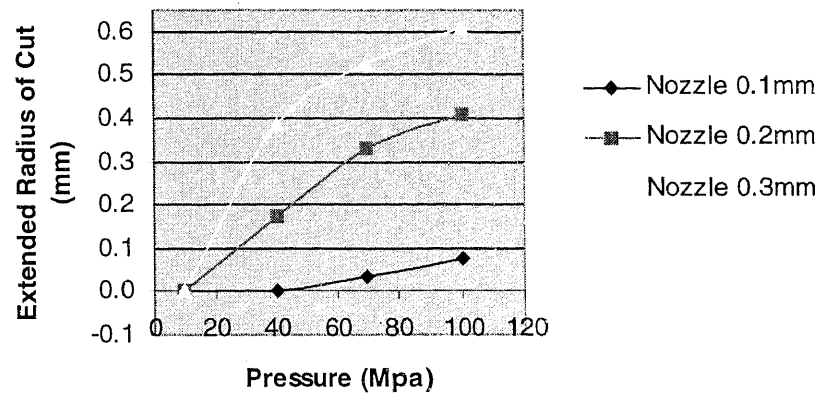


Figure 6-5 The relationship between the pressure and the extended radius of cut.

Relationship between Pressure and Depth of Cut

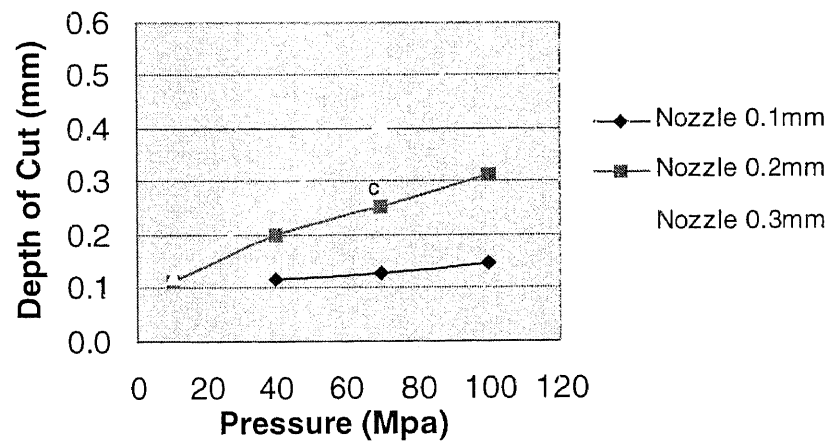


Figure 6-6 The relationship between the pressure and the depth of cut based on the nozzle sizes

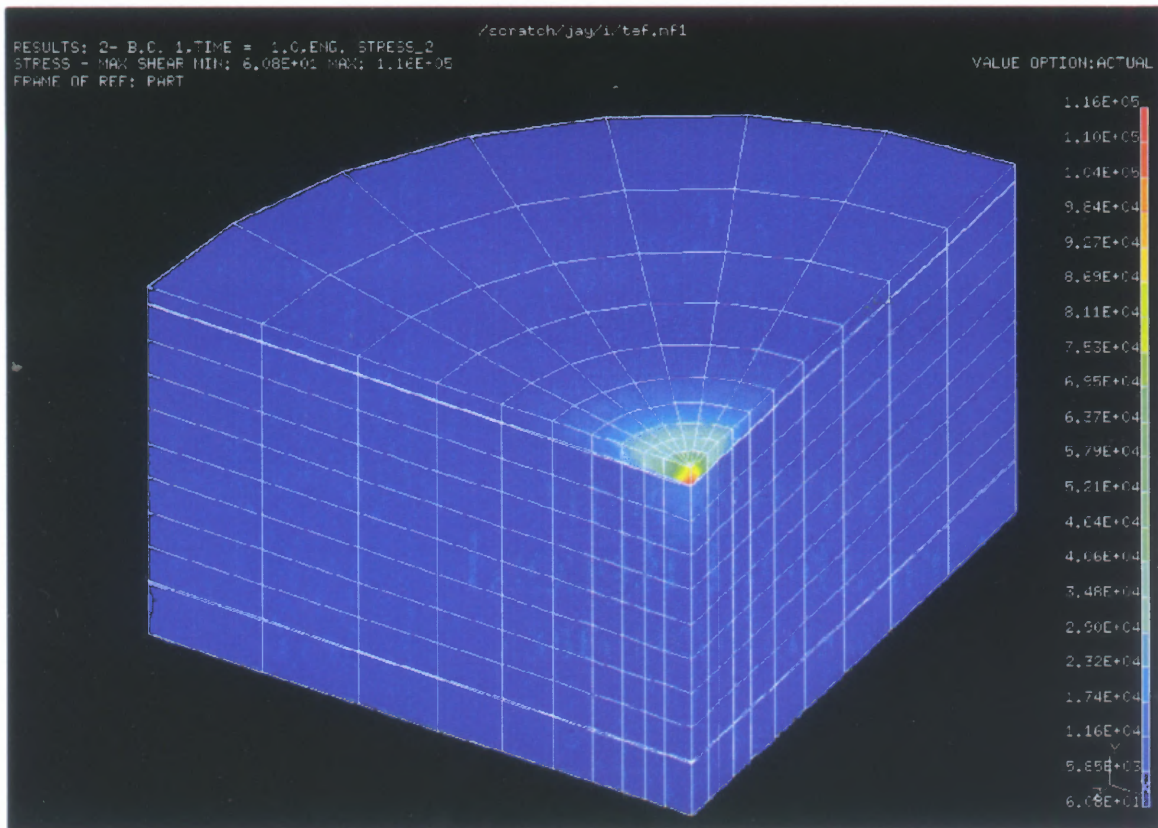


Figure 6-7 The contour plot of stress shows the stress distribution. The maximum value is on the corner of epidermis layer without deformation.

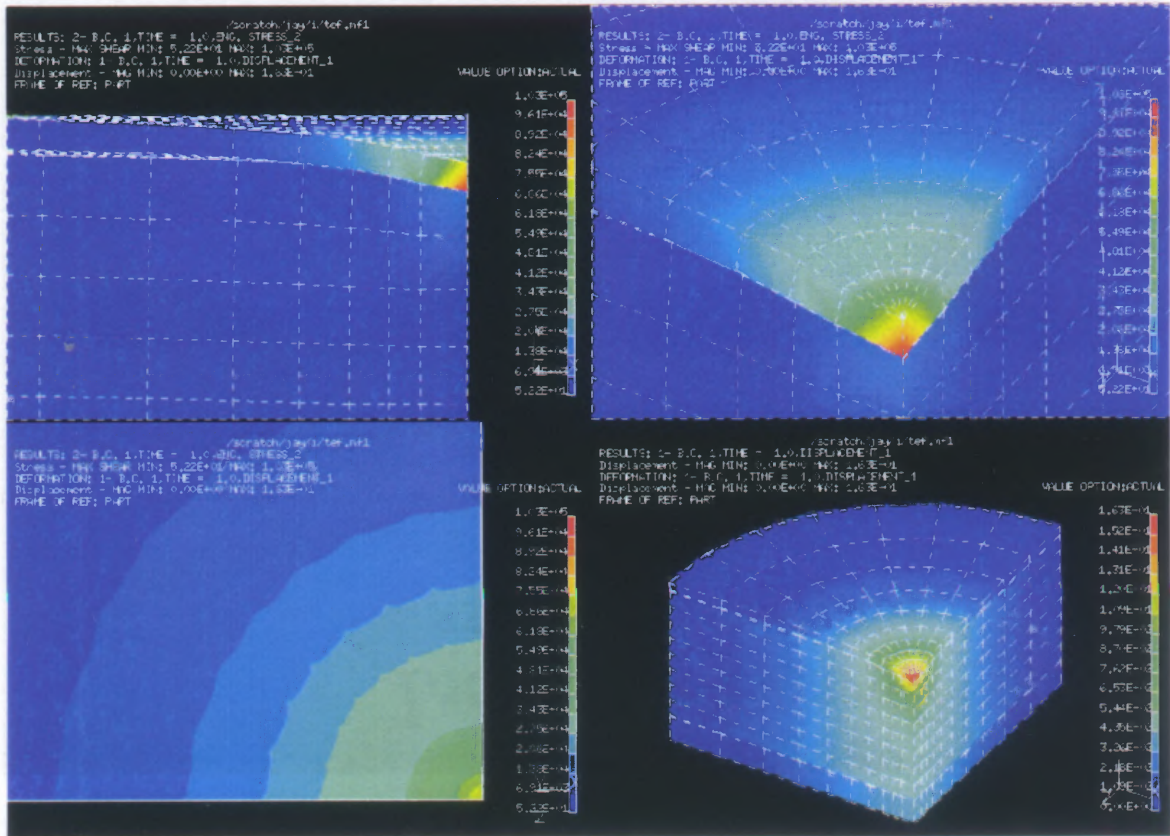


Figure 6-8 The contour plots show the displacement and deformation.

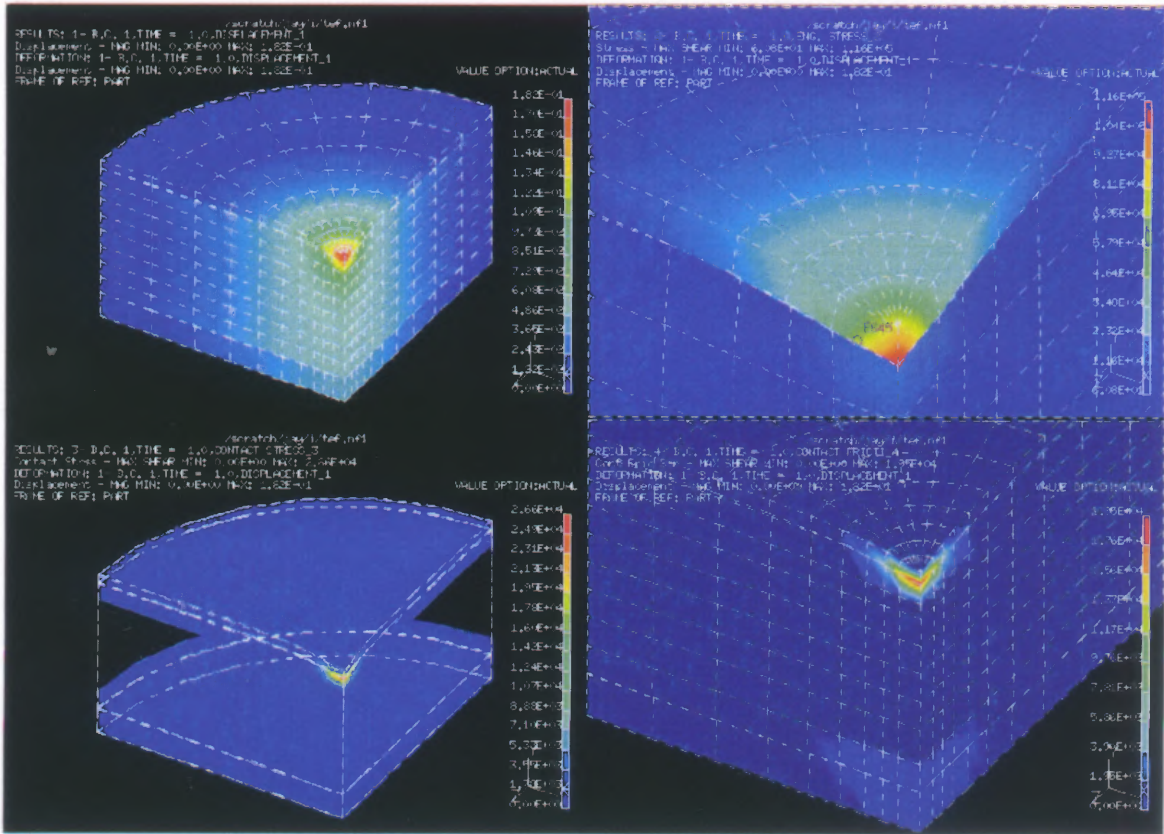


Figure 6-9 The contour plots show the area of contact stress and contact pressure. 10MPa

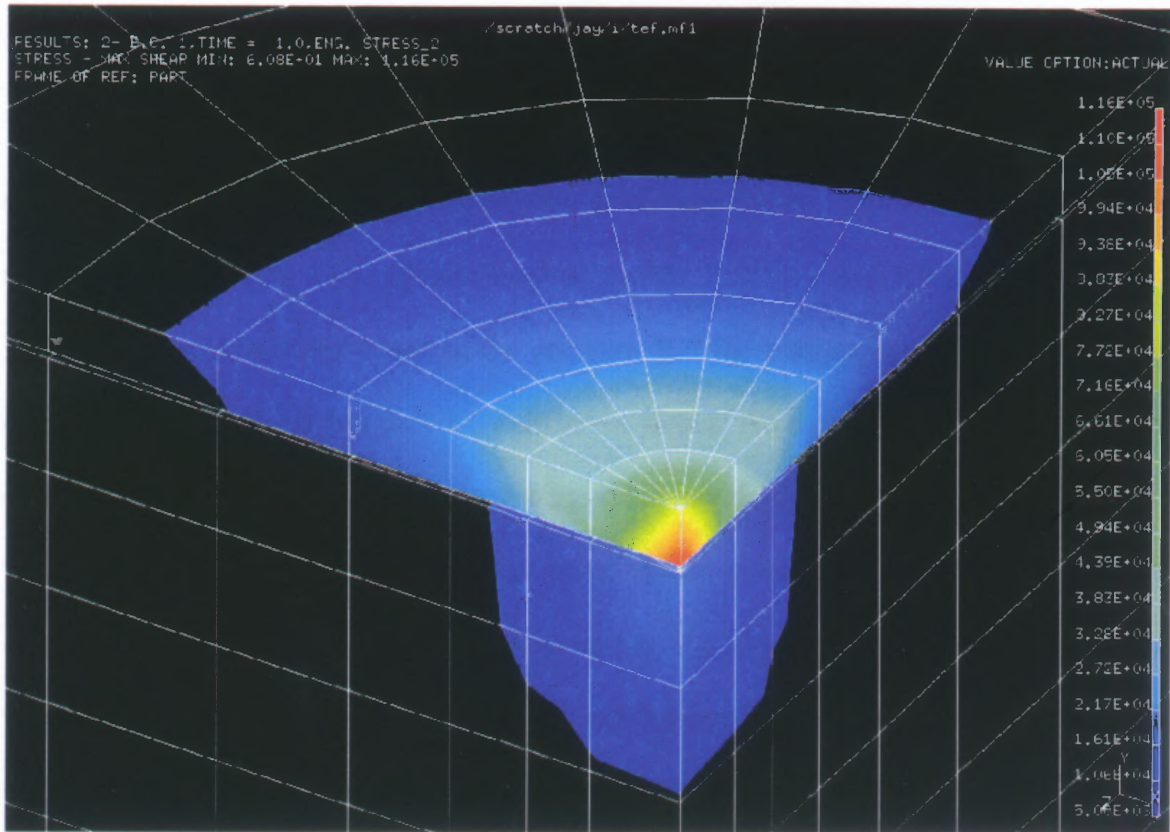


Figure 6-10 The contour plot shows the area that has stress value from 5MPa to 10MPa. This area will shear and be removed from the skin.

Table 7-4 The elements that have with maximum stress and their parameters

Relationship between elements and stress	Topology	X	Y	Z	Max
Element 1	Element 1	0.1021	0.1021	0.1021	1
Element 2	Element 2	0.1021	0.1021	0.1021	2
Element 3	Element 3	0.1021	0.1021	0.1021	3
Relationship between element and displacement	Topology	X	Y	Z	Max
Element 1	Element 1	0.1021	0.1021	0.1021	1
Element 2	Element 2	0.1021	0.1021	0.1021	2
Element 3	Element 3	0.1021	0.1021	0.1021	3

The relationship between the elements and stress and displacement is shown in Table 7-4. It shows that the maximum stress and displacement are in the same element.

CHAPTER 7

ANALYSIS OF RESULTS

Curve fitting method is used to identify the governing equations of relationship between the cutting parameters. From the results shown in the Table 6-5 and the graphs on Figures 3 and 4, the relationships between the pressure and the maximum shear stress and the displacement, are linear but they have different slopes. As shown in Table 7-1 (X in the equations represents the pressure), the bigger the nozzle diameter the higher the slope. Thus, the nozzle cannot generate adequate shear stress on the skin, even under considerably high pressure, if its diameter is not big enough. The relationship between the pressure and the extended radius of cut and the depth of cut, are not linear, as shown in Figures 5 and 6, respectively. The developed governing functions for different nozzle diameters do not show any correlation among them.

Table 7-1 The equations that represent relationship between cutting parameters.

Relationship between pressure and stress	Equation	a	b	R²	Rank
P-S, nozzle 0.1mm	Eqn 1 $y=a+bx$	-0.110333	0.20273333	0.999999027	3
P-S, nozzle 0.2mm	Eqn 1 $y=a+bx$	0.283333	0.57066667	0.999988673	4
P-S, nozzle 0.3mm	Eqn 1 $y=a+bx$	0.217333	0.93936667	0.999997917	
Relationship between pressure and displacement	Equation	a	b	R²	Rank
P-D, nozzle 0.1mm	Eqn 1 $y=a+bx$	0.009767	0.000213333	0.99902439	3
P-D, nozzle 0.2mm	Eqn 1 $y=a+bx$	0.012667	0.000883333	0.997868561	10
P-D, nozzle 0.3mm	Eqn 1 $y=a+bx$	0.014433	0.001596667	0.999416313	4

For the relationship between the extended radius and the depth of cut, the governing equation is found nonlinear. It shows that at the small value of pressure, The maximum stress is considerably lower than the ultimate tensile strength of the epidermis

and the jet generates a cut horizontally instead of vertically. But once the pressure is high enough to exceed the strength of epidermis. The jet will now provide a vertically cut.

The graph below represents the relationship between extended radius of cut and depth of cut obtained from curve fitting method by using TableCurve. The set of data between extended radius of cut and depth of cut for each analysis number was imported into the program. The program provided a fifth order polynomial equation. This equation can be used to intrapolate the width or depth of cut based on the cutting parameters in this research.

governing equation of the relationship between extended radius of cut and

Rank 9 Eqn 6002

$$Y=a+bx+cx^2+dx^3+ex^4+fx^5$$

$R^2=0.959162242$ a=0.0878 b=1.196 c=-5.6410 d=17.6574 e=-27.8223 f=20.2398

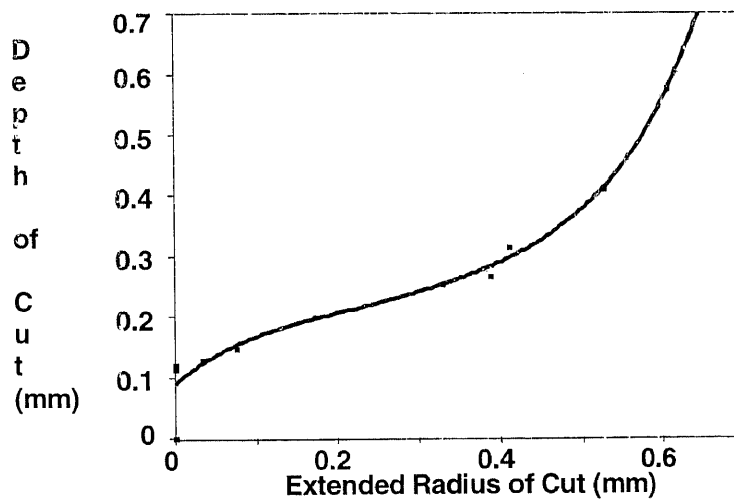


Figure 7-1 The relationship of the radius and depth of cut.

CHAPTER 8

CONCLUSIONS AND RECOMMENDATIONS

The nozzle diameter of 0.1mm could not generate required shear stress on the skin, especially the epidermis layer, which has the highest Young's modulus and is the stiffest layer among the three. Epidermis acts like a shield, protecting the tissue underneath. In order to cut through this layer, The force generated by the jet stream must be high enough to exceed the ultimate tensile stress of the epidermis. We all know that the higher the pressure, the higher the force is. But, if the pressure in the reservoir is constant, the higher force is obtained from the bigger nozzle diameter. The cutting condition at the pressure of 40MPa with 0.2mm nozzle diameter was found to generate optimum depth and width of cut. A width of cut of 0.3mm and a depth of incision on the skin of 0.5mm, are generated. Although, the generated depth is considerably small and cannot cut through the skin in one pass, but the width is suitable for cutting and it should be reduced as needed. A multiple pass can be used on this size of nozzle to provide a deeper cut on the skin, The 0.3mm nozzle provides the deepest cutting but it also generates 1.2mm width of cut on the epidermis layer, which is unacceptable.

The relationship among the parameters shows that pressure and nozzle diameter influence the character of water jet cutting. On the other hand, stand-off distance and flare angle constant almost cause a slightly effect on the skin cutting.

The friction gaps between layers also show an effect on the skin cutting. The air gaps provide a resistant against the jet stream penetrating from epidermis layer to dermis layer. The cutting force is absorbed and distributed away, through out the contact surface other than cutting the layer underneath.

APPENDIX A

RESULTS OF ANALYSIS

1. The stress value on nodes

1. Stress values of nodes number 1-11 along the edge of the top surface (radius).
2. Stress values of nodes number 1-13 along the vertical edge that passes through the axis (center) of the model.

The first column represents node number. The second column represents the distance measures from the origin to each node (mm). The third column represents the stress value of each node (kPa)

Solution48			Solution47, 46			Solution45		
1	0.000	94180.0	1	0.000	94140.0	1	0.000	94110.0
2	0.150	36290.0	2	0.150	36280.0	2	0.150	36270.0
3	0.257	36420.0	3	0.257	36410.0	3	0.257	36400.0
4	0.387	24210.0	4	0.387	24200.0	4	0.387	24200.0
5	0.557	12850.0	5	0.557	12850.0	5	0.557	12850.0
6	0.778	6306.0	6	0.778	6303.0	6	0.778	6301.0
7	1.064	3096.0	7	1.064	3095.0	7	1.064	3094.0
8	1.424	1467.0	8	1.424	1467.0	8	1.424	1467.0
9	1.868	626.0	9	1.868	625.8	9	1.868	625.6
10	2.407	190.3	10	2.407	190.3	10	2.407	190.3
11	3.000	52.3	11	3.000	52.1	11	3.000	52.1
Solution48			Solution47, 46			Solution45		
1	0.000	94180.0	1	0.000	94140.0	1	0.000	94110.0
2	0.100	128000.0	2	0.100	128000.0	2	0.100	127900.0
3	0.110	17750.0	3	0.110	17740.0	3	0.110	17730.0
4	0.310	11710.0	4	0.310	11710.0	4	0.310	11710.0
5	0.510	5451.0	5	0.510	5449.0	5	0.510	5447.0
6	0.710	3344.0	6	0.710	3343.0	6	0.710	3342.0
7	0.910	2194.0	7	0.910	2193.0	7	0.910	2193.0
8	1.110	1590.0	8	1.110	1590.0	8	1.110	1589.0
9	1.310	1210.0	9	1.310	1209.0	9	1.310	1209.0
10	1.510	1065.0	10	1.510	1065.0	10	1.510	1064.0
11	1.710	1034.0	11	1.710	1034.0	11	1.710	1033.0
12	1.720	363.0	12	1.720	362.8	12	1.720	362.7
13	2.020	278.7	13	2.020	278.5	13	2.020	278.4
Solution44			Solution43, 42			Solution41		
1	0.000	57305.00	1	0.000	57300.0	1	0.000	57290.0
2	0.100	27683.00	2	0.100	27680.0	2	0.100	27670.0
3	0.207	23160.00	3	0.207	23150.0	3	0.207	23140.0
4	0.337	13700.00	4	0.337	13700.0	4	0.337	13690.0
5	0.507	6760.00	5	0.507	6759.0	5	0.507	6757.0
6	0.728	3199.00	6	0.728	3194.0	6	0.728	3193.0
7	1.014	1573.00	7	1.014	1573.0	7	1.014	1573.0
8	1.374	790.00	8	1.374	789.4	8	1.374	789.2
9	1.819	388.00	9	1.819	388.0	9	1.819	388.0
10	2.358	178.60	10	2.358	178.6	10	2.358	178.6
11	3.000	117.10	11	3.000	117.1	11	3.000	117.2

Solution	43,42		Solution43, 42		Solution41	
	1	0.000	57305.00	1	0.000	57300.0
	2	0.100	96713.00	2	0.100	96700.0
	3	0.110	10566.00	3	0.110	10560.0
	4	0.310	6010.00	4	0.310	6001.0
	5	0.510	2442.00	5	0.510	2439.0
	6	0.710	1553.00	6	0.710	1562.0
	7	0.910	974.00	7	0.910	975.3
	8	1.110	730.00	8	1.110	729.5
	9	1.310	561.00	9	1.310	559.4
	10	1.510	492.50	10	1.510	492.2
	11	1.710	463.80	11	1.710	463.2
	12	1.720	172.9	12	1.720	172.5
	13	2.020	109.80	13	2.020	109.8
Solution	40		Solution39, 38		Solution37	
	1	0.000	20170.0	1	0.000	20170.0
	2	0.050	12294.0	2	0.050	12290.0
	3	0.159	5693.0	3	0.159	5691.0
	4	0.291	2914.0	4	0.291	2913.0
	5	0.464	1398.0	5	0.464	1396.0
	6	0.689	674.1	6	0.689	673.1
	7	0.980	373.9	7	0.980	373.7
	8	1.346	236.0	8	1.346	235.9
	9	1.799	168.0	9	1.799	167.3
	10	2.347	132.6	10	2.347	132.4
	11	3.000	141.4	11	3.000	141.7
Solution	40		Solution39, 38		Solution37	
	1	0.000	20170.0	1	0.000	20170.0
	2	0.100	41922.0	2	0.100	41880.0
	3	0.110	1844.0	3	0.110	1842.0
	4	0.310	994.0	4	0.310	993.7
	5	0.510	505.6	5	0.510	504.4
	6	0.710	231.2	6	0.710	230.7
	7	0.910	159.6	7	0.910	159.6
	8	1.110	90.3	8	1.110	90.1
	9	1.310	73.8	9	1.310	73.6
	10	1.510	63.3	10	1.510	64.3
	11	1.710	96.6	11	1.710	96.0
	12	1.720	0.0	12	1.720	0.0
	13	2.020	0.0	13	2.020	0.0
Solution36			Solution35, 34		Solution33	
	1	0.000	65970.0	1	0.000	65940.0
	2	0.150	25470.0	2	0.150	25450.0
	3	0.257	25480.0	3	0.257	25470.0
	4	0.387	16880.0	4	0.387	16870.0
	5	0.557	8967.0	5	0.557	8963.0
	6	0.778	4437.0	6	0.778	4435.0
	7	1.064	2218.0	7	1.064	2217.0
	8	1.424	1090.0	8	1.424	1090.0
	9	1.868	497.1	9	1.868	497.0
	10	2.407	191.8	10	2.407	191.8
	11	3.000	58.7	11	3.000	58.8
Solution36			Solution35, 34		Solution33	
	1	0.000	65970.0	1	0.000	65920.0
	2	0.100	89630.0	2	0.100	89560.0
	3	0.110	12390.0	3	0.110	12380.0
	4	0.310	8177.0	4	0.310	8171.0
	5	0.510	3787.0	5	0.510	3784.0
	6	0.710	2322.0	6	0.710	2320.0
	7	0.910	1534.0	7	0.910	1533.0
	8	1.110	1124.0	8	1.110	1123.0
	9	1.310	878.6	9	1.310	878.1
	10	1.510	760.6	10	1.510	760.1
	11	1.710	679.4	11	1.710	678.9
	12	1.720	213.9	12	1.720	213.6
	13	2.020	151.7	13	2.020	151.5

Solution32			Solution31, 30			Solution29		
1	0.000	40240.0	1	0.000	40220.0	1	0.000	40210.0
2	0.100	19440.0	2	0.100	19430.0	2	0.100	19430.0
3	0.207	16240.0	3	0.207	16240.0	3	0.207	16230.0
4	0.337	9589.0	4	0.337	9585.0	4	0.337	9583.0
5	0.507	4758.0	5	0.507	4756.0	5	0.507	4755.0
6	0.728	2280.0	6	0.728	2279.0	6	0.728	2278.0
7	1.014	1153.0	7	1.014	1152.0	7	1.014	1152.0
8	1.374	607.7	8	1.374	607.5	8	1.374	607.4
9	1.819	327.7	9	1.819	327.6	9	1.819	327.6
10	2.358	177.3	10	2.358	177.3	10	2.358	177.3
11	3.000	150.9	11	3.000	150.9	11	3.000	150.9
Solution32			Solution31, 30			Solution29		
1	0.000	40240.0	1	0.000	40220.0	1	0.000	40210.0
2	0.100	67890.0	2	0.100	67860.0	2	0.100	67840.0
3	0.110	7314.0	3	0.110	7310.0	3	0.110	7308.0
4	0.310	4189.0	4	0.310	4187.0	4	0.310	4186.0
5	0.510	1694.0	5	0.510	1693.0	5	0.510	1693.0
6	0.710	1073.0	6	0.710	1073.0	6	0.710	1072.0
7	0.910	665.0	7	0.910	664.7	7	0.910	664.5
8	1.110	504.1	8	1.110	503.8	8	1.110	503.7
9	1.310	398.4	9	1.310	398.3	9	1.310	398.2
10	1.510	360.1	10	1.510	359.9	10	1.510	359.8
11	1.710	360.0	11	1.710	359.7	11	1.710	359.5
12	1.720	166.1	12	1.720	166.0	12	1.720	165.9
13	2.020	104.8	13	2.020	104.7	13	2.020	104.6
Solution28			Solution26, 27			Solution25		
1	0.000	14070.0	1	0.000	14070.0	1	0.000	14070.0
2	0.050	8671.0	2	0.050	8670.0	2	0.050	8668.0
3	0.159	4029.0	3	0.159	4028.0	3	0.159	4027.0
4	0.291	2063.0	4	0.291	2063.0	4	0.291	2062.0
5	0.464	1008.0	5	0.464	1008.0	5	0.464	1008.0
6	0.689	502.1	6	0.689	502.0	6	0.689	502.0
7	0.980	292.8	7	0.980	292.8	7	0.980	292.7
8	1.346	196.4	8	1.346	196.4	8	1.346	196.4
9	1.799	148.4	9	1.799	148.4	9	1.799	148.4
10	2.347	124.5	10	2.347	124.5	10	2.347	124.5
11	3.000	136.1	11	3.000	136.1	11	3.000	136.1
Solution28			Solution26, 27			Solution25		
1	0.000	14070.0	1	0.000	14070.0	1	0.000	14070.0
2	0.100	29530.0	2	0.100	29530.0	2	0.100	29520.0
3	0.110	1209.0	3	0.110	1209.0	3	0.110	1209.0
4	0.310	721.6	4	0.310	721.5	4	0.310	721.4
5	0.510	363.9	5	0.510	363.9	5	0.510	363.8
6	0.710	160.5	6	0.710	160.5	6	0.710	160.5
7	0.910	114.3	7	0.910	114.3	7	0.910	114.3
8	1.110	62.5	8	1.110	62.5	8	1.110	62.5
9	1.310	52.2	9	1.310	52.2	9	1.310	52.2
10	1.510	44.8	10	1.510	44.8	10	1.510	44.8
11	1.710	68.4	11	1.710	68.4	11	1.710	68.4
12	1.720	0.0	12	1.720	0.0	12	1.720	0.0
13	2.020	0.0	13	2.020	0.0	13	2.020	0.0
Solution24			Solution23, 22			Solution21		
1	0.000	37720.0	1	0.000	37710.0	1	0.000	37700.0
2	0.150	14560.0	2	0.150	14550.0	2	0.150	14550.0
3	0.257	14540.0	3	0.257	14530.0	3	0.257	14530.0
4	0.387	9602.0	4	0.387	9598.0	4	0.387	9596.0
5	0.557	5145.0	5	0.557	5142.0	5	0.557	5141.0
6	0.778	2593.0	6	0.778	2592.0	6	0.778	2591.0
7	1.064	1342.0	7	1.064	1341.0	7	1.064	1341.0
8	1.424	705.2	8	1.424	705.0	8	1.424	704.9
9	1.868	367.4	9	1.868	367.4	9	1.868	367.3
10	2.407	183.9	10	2.407	183.9	10	2.407	183.9
11	3.000	139.0	11	3.000	139.0	11	3.000	139.1

Solution24			Solution23, 22			Solution21		
1	0.000	37720.0	1	0.000	37710.0	1	0.000	37700.0
2	0.100	51210.0	2	0.100	51190.0	2	0.100	51170.0
3	0.110	7037.0	3	0.110	7033.0	3	0.110	7032.0
4	0.310	4629.0	4	0.310	4627.0	4	0.310	4626.0
5	0.510	2140.0	5	0.510	2139.0	5	0.510	2139.0
6	0.710	1305.0	6	0.710	1305.0	6	0.710	1305.0
7	0.910	861.0	7	0.910	860.6	7	0.910	860.4
8	1.110	636.6	8	1.110	636.3	8	1.110	636.2
9	1.310	500.5	9	1.310	500.3	9	1.310	500.2
10	1.510	444.1	10	1.510	443.9	10	1.510	443.9
11	1.710	426.3	11	1.710	426.2	11	1.710	426.2
12	1.720	156.4	12	1.720	156.4	12	1.720	156.4
13	2.020	101.9	13	2.020	101.9	13	2.020	101.9
Solution 20			Solution19, 18			Solution17		
1	0.000	23210.0	1	0.000	23200.0	1	0.000	23190.0
2	0.100	11190.0	2	0.100	11180.0	2	0.100	11180.0
3	0.207	9341.0	3	0.207	9337.0	3	0.207	9335.0
4	0.337	5513.0	4	0.337	5510.0	4	0.337	5509.0
5	0.507	2772.0	5	0.507	2771.0	5	0.507	2770.0
6	0.728	1363.0	6	0.728	1362.0	6	0.728	1362.0
7	1.014	722.1	7	1.014	721.8	7	1.014	721.6
8	1.374	411.8	8	1.374	411.6	8	1.374	411.6
9	1.819	252.0	9	1.819	252.0	9	1.819	252.0
10	2.358	166.5	10	2.358	166.5	10	2.358	166.4
11	3.000	163.7	11	3.000	163.7	11	3.000	163.7
Solution 20			Solution19, 18			Solution17		
1	0.000	23210.0	1	0.000	23200.0	1	0.000	23190.0
2	0.100	39140.0	2	0.100	39130.0	2	0.100	39120.0
3	0.110	4054.0	3	0.110	4052.0	3	0.110	4051.0
4	0.310	2392.0	4	0.310	2391.0	4	0.310	2391.0
5	0.510	965.9	5	0.510	965.5	5	0.510	965.3
6	0.710	582.7	6	0.710	582.5	6	0.710	582.3
7	0.910	338.5	7	0.910	338.3	7	0.910	338.2
8	1.110	228.0	8	1.110	227.9	8	1.110	227.8
9	1.310	166.8	9	1.310	166.7	9	1.310	166.6
10	1.510	162.0	10	1.510	161.6	10	1.510	161.4
11	1.710	212.4	11	1.710	212.1	11	1.710	211.9
12	1.720	6.1	12	1.720	5.6	12	1.720	5.3
13	2.020	5.7	13	2.020	5.2	13	2.020	5.0
Solution16			Solution15, 14			Solution13		
1	0.000	7995.0	1	0.000	7991.0	1	0.000	7989.0
2	0.050	4966.0	2	0.050	4963.0	2	0.050	4962.0
3	0.159	2325.0	3	0.159	2324.0	3	0.159	2323.0
4	0.291	1163.0	4	0.291	1162.0	4	0.291	1162.0
5	0.464	584.4	5	0.464	584.2	5	0.464	584.0
6	0.689	318.8	6	0.689	318.7	6	0.689	318.7
7	0.980	208.7	7	0.980	208.7	7	0.980	208.6
8	1.346	157.7	8	1.346	157.6	8	1.346	157.6
9	1.799	132.1	9	1.799	132.1	9	1.799	132.1
10	2.347	120.3	10	2.347	120.3	10	2.347	120.3
11	3.000	134.9	11	3.000	134.9	11	3.000	134.9
Solution16			Solution15, 14			Solution13		
1	0.000	7995.0	1	0.000	7991.0	1	0.000	7989.0
2	0.100	16850.0	2	0.100	16840.0	2	0.100	16830.0
3	0.110	674.1	3	0.110	673.8	3	0.110	673.6
4	0.310	419.0	4	0.310	418.8	4	0.310	418.7
5	0.510	208.2	5	0.510	208.1	5	0.510	208.0
6	0.710	87.3	6	0.710	87.2	6	0.710	87.2
7	0.910	66.1	7	0.910	66.1	7	0.910	66.1
8	1.110	34.1	8	1.110	34.1	8	1.110	34.0
9	1.310	29.9	9	1.310	29.9	9	1.310	29.9
10	1.510	25.0	10	1.510	25.0	10	1.510	25.0
11	1.710	39.8	11	1.710	39.8	11	1.710	39.7
12	1.720	0.0	12	1.720	0.0	12	1.720	0.0
13	2.020	0.0	13	2.020	0.0	13	2.020	0.0

Solution12			Solution11, 10			Solution9		
1	0.000	9656.0	1	0.000	9652.0	1	0.000	9650.0
2	0.150	3701.0	2	0.150	3699.0	2	0.150	3698.0
3	0.257	3646.0	3	0.257	3644.0	3	0.257	3643.0
4	0.387	2364.0	4	0.387	2363.0	4	0.387	2362.0
5	0.557	1309.0	5	0.557	1308.0	5	0.557	1308.0
6	0.778	713.4	6	0.778	713.0	6	0.778	712.9
7	1.064	421.3	7	1.064	421.1	7	1.064	421.1
8	1.424	272.2	8	1.424	272.2	8	1.424	272.1
9	1.868	192.6	9	1.868	192.5	9	1.868	192.5
10	2.407	149.9	10	2.407	149.8	10	2.407	149.8
11	3.000	157.9	11	3.000	157.9	11	3.000	157.9
Solution12			Solution11, 10			Solution9		
1	0.000	9656.0	1	0.000	9652.0	1	0.000	9650.0
2	0.100	13070.0	2	0.100	13060.0	2	0.100	13060.0
3	0.110	1672.0	3	0.110	1671.0	3	0.110	1671.0
4	0.310	1154.0	4	0.310	1153.0	4	0.310	1153.0
5	0.510	536.2	5	0.510	535.9	5	0.510	535.8
6	0.710	306.6	6	0.710	306.5	6	0.710	306.4
7	0.910	188.0	7	0.910	188.0	7	0.910	187.9
8	1.110	124.7	8	1.110	124.7	8	1.110	124.6
9	1.310	93.1	9	1.310	93.0	9	1.310	93.0
10	1.510	88.3	10	1.510	88.2	10	1.510	88.2
11	1.710	116.0	11	1.710	115.9	11	1.710	115.9
12	1.720	0.0	12	1.720	0.0	12	1.720	0.0
13	2.020	0.0	13	2.020	0.0	13	2.020	0.0
Solution8			Solution7, 6			Solution5		
1	0.000	5919.0	1	0.000	5916.0	1	0.000	5915.0
2	0.100	2831.0	2	0.100	2830.0	2	0.100	2829.0
3	0.207	2363.0	3	0.207	2362.0	3	0.207	2362.0
4	0.337	1353.0	4	0.337	1353.0	4	0.337	1352.0
5	0.507	715.1	5	0.507	714.8	5	0.507	714.6
6	0.728	397.0	6	0.728	396.9	6	0.728	396.8
7	1.014	252.3	7	1.014	252.2	7	1.014	252.2
8	1.374	182.0	8	1.374	181.9	8	1.374	181.9
9	1.819	145.6	9	1.819	145.6	9	1.819	145.6
10	2.358	127.5	10	2.358	127.5	10	2.358	127.5
11	3.000	141.2	11	3.000	141.2	11	3.000	141.2
Solution8			Solution7, 6			Solution5		
1	0.000	5919.0	1	0.000	5916.0	1	0.000	5915.0
2	0.100	9937.0	2	0.100	9932.0	2	0.100	9930.0
3	0.110	954.1	3	0.110	953.6	3	0.110	953.4
4	0.310	615.3	4	0.310	615.0	4	0.310	614.9
5	0.510	256.8	5	0.510	256.6	5	0.510	256.6
6	0.710	144.2	6	0.710	144.1	6	0.710	144.1
7	0.910	85.9	7	0.910	85.9	7	0.910	85.9
8	1.110	56.5	8	1.110	56.5	8	1.110	56.5
9	1.310	41.5	9	1.310	41.5	9	1.310	41.5
10	1.510	39.3	10	1.510	39.2	10	1.510	39.2
11	1.710	52.0	11	1.710	52.0	11	1.710	52.0
12	1.720	0.0	12	1.720	0.0	12	1.720	0.0
13	2.020	0.0	13	2.020	0.0	13	2.020	0.0
Solution4			Solution2, 3			Solution1		
1	0.000	1921.0	1	0.000	1920.0	1	0.000	1920.0
2	0.050	1304.0	2	0.050	1304.0	2	0.050	1304.0
3	0.159	681.9	3	0.159	681.6	3	0.159	681.5
4	0.291	393.2	4	0.291	393.1	4	0.291	393.1
5	0.464	272.8	5	0.464	272.8	5	0.464	272.8
6	0.689	199.4	6	0.689	199.4	6	0.689	199.4
7	0.980	143.3	7	0.980	143.3	7	0.980	143.3
8	1.346	118.7	8	1.346	118.7	8	1.346	118.7
9	1.799	114.3	9	1.799	114.3	9	1.799	114.3
10	2.347	113.8	10	2.347	113.8	10	2.347	113.8
11	3.000	130.9	11	3.000	130.9	11	3.000	130.9

Solution4			Solution2, 3			Solution1		
1	0.000	1921.0	1	0.000	1920.0	1	0.000	1920.0
2	0.100	4291.0	2	0.100	4289.0	2	0.100	4288.0
3	0.110	94.2	3	0.110	94.1	3	0.110	94.1
4	0.310	129.8	4	0.310	129.7	4	0.310	129.7
5	0.510	62.0	5	0.510	62.0	5	0.510	62.0
6	0.710	16.3	6	0.710	16.3	6	0.710	16.3
7	0.910	19.6	7	0.910	19.6	7	0.910	19.6
8	1.110	6.3	8	1.110	6.3	8	1.110	6.3
9	1.310	8.2	9	1.310	8.2	9	1.310	8.1
10	1.510	5.4	10	1.510	5.4	10	1.510	5.4
11	1.710	11.7	11	1.710	11.7	11	1.710	11.7
12	1.720	0.0	12	1.720	0.0	12	1.720	0.0
13	2.020	0.0	13	2.020	0.0	13	2.020	0.0

2. The displacement value on nodes

1. Displacement values of nodes number 1-11 along the edge of the top surface (radius).
2. Displacement values of nodes number 1-13 along the vertical edge that passes through the axis (center) of the model.

The first column represents node numbers. The second column represents the distance measures from the origin to each node (mm). The third column represents the displacement values of each node (mm)

Solution48			Solution47, 46			Solution45		
1	0.000	0.173000	1	0.000	0.173000	1	0.000	0.172900
2	0.150	0.135700	2	0.150	0.135600	2	0.150	0.135600
3	0.257	0.102200	3	0.257	0.102100	3	0.257	0.102100
4	0.387	0.072510	4	0.387	0.072490	4	0.387	0.072470
5	0.557	0.047740	5	0.557	0.047730	5	0.557	0.047720
6	0.778	0.027940	6	0.778	0.027940	6	0.778	0.027940
7	1.064	0.013230	7	1.064	0.013230	7	1.064	0.013230
8	1.424	0.003955	8	1.424	0.003957	8	1.424	0.003959
9	1.868	0.000442	9	1.868	0.000440	9	1.868	0.000440
10	2.407	0.000601	10	2.407	0.000600	10	2.407	0.000600
11	3.000	0.000000	11	3.000	0.000000	11	3.000	0.000000

Solution48			Solution47, 46			Solution45		
1	0.000	0.173000	1	0.000	0.173000	1	0.000	0.172900
2	0.100	0.163200	2	0.100	0.163200	2	0.100	0.163100
3	0.110	0.153200	3	0.110	0.153100	3	0.110	0.153100
4	0.310	0.085900	4	0.310	0.085870	4	0.310	0.085850
5	0.510	0.060160	5	0.510	0.060140	5	0.510	0.060120
6	0.710	0.044680	6	0.710	0.044660	6	0.710	0.044650
7	0.910	0.035140	7	0.910	0.035130	7	0.910	0.035130
8	1.110	0.028600	8	1.110	0.028590	8	1.110	0.028590
9	1.310	0.023730	9	1.310	0.023730	9	1.310	0.023720
10	1.510	0.020150	10	1.510	0.020150	10	1.510	0.020140
11	1.710	0.016310	11	1.710	0.016310	11	1.710	0.016310
12	1.720	0.006384	12	1.720	0.006381	12	1.720	0.006379
13	2.020	0.003802	13	2.020	0.003800	13	2.020	0.003800

Solution44			Solution43, 42			Solution41		
1	0.000	0.099870	1	0.000	0.099870	1	0.000	0.099850
2	0.100	0.082520	2	0.100	0.082520	2	0.100	0.082500
3	0.207	0.062720	3	0.207	0.062720	3	0.207	0.062710
4	0.337	0.046340	4	0.337	0.046340	4	0.337	0.046340
5	0.507	0.033000	5	0.507	0.033000	5	0.507	0.033000
6	0.728	0.022140	6	0.728	0.022140	6	0.728	0.022140
7	1.014	0.013460	7	1.014	0.013460	7	1.014	0.013460
8	1.374	0.007011	8	1.374	0.007011	8	1.374	0.007012
9	1.819	0.002793	9	1.819	0.002793	9	1.819	0.002793
10	2.358	0.000624	10	2.358	0.000624	10	2.358	0.000624
11	3.000	0.000000	11	3.000	0.000000	11	3.000	0.000000
Solution44			Solution43, 42			Solution41		
1	0.000	0.099870	1	0.000	0.099870	1	0.000	0.099850
2	0.100	0.090290	2	0.100	0.090290	2	0.100	0.090270
3	0.110	0.081000	3	0.110	0.081000	3	0.110	0.080980
4	0.310	0.043310	4	0.310	0.043310	4	0.310	0.043300
5	0.510	0.032410	5	0.510	0.032410	5	0.510	0.032400
6	0.710	0.024860	6	0.710	0.024860	6	0.710	0.024850
7	0.910	0.020730	7	0.910	0.020730	7	0.910	0.020730
8	1.110	0.017780	8	1.110	0.017780	8	1.110	0.017780
9	1.310	0.015660	9	1.310	0.015660	9	1.310	0.015650
10	1.510	0.014070	10	1.510	0.014070	10	1.510	0.014070
11	1.710	0.012520	11	1.710	0.012520	11	1.710	0.012520
12	1.720	0.002350	12	1.720	0.002350	12	1.720	0.002349
13	2.020	0.000993	13	2.020	0.000993	13	2.020	0.000992
Solution40			Solution39, 38			Solution37		
1	0.000	0.030840	1	0.000	0.030820	1	0.000	0.030790
2	0.050	0.025880	2	0.050	0.025850	2	0.050	0.025830
3	0.159	0.021840	3	0.159	0.021820	3	0.159	0.021800
4	0.291	0.018110	4	0.291	0.018110	4	0.291	0.018110
5	0.464	0.014920	5	0.464	0.014920	5	0.464	0.014920
6	0.689	0.011930	6	0.689	0.011930	6	0.689	0.011940
7	0.980	0.008937	7	0.980	0.008937	7	0.980	0.008949
8	1.346	0.005952	8	1.346	0.005955	8	1.346	0.005966
9	1.799	0.003152	9	1.799	0.003152	9	1.799	0.003159
10	2.347	0.000934	10	2.347	0.000934	10	2.347	0.000936
11	3.000	0.000000	11	3.000	0.000000	11	3.000	0.000000
Solution40			Solution39, 38			Solution37		
1	0.000	0.030840	1	0.000	0.030820	1	0.000	0.030790
2	0.100	0.024860	2	0.100	0.024830	2	0.100	0.024800
3	0.110	0.015110	3	0.110	0.015090	3	0.110	0.015070
4	0.310	0.009520	4	0.310	0.009500	4	0.310	0.009482
5	0.510	0.006651	5	0.510	0.006645	5	0.510	0.006639
6	0.710	0.005770	6	0.710	0.005770	6	0.710	0.005764
7	0.910	0.004906	7	0.910	0.004903	7	0.910	0.004900
8	1.110	0.004638	8	1.110	0.004634	8	1.110	0.004630
9	1.310	0.004345	9	1.310	0.004342	9	1.310	0.004339
10	1.510	0.004270	10	1.510	0.004267	10	1.510	0.004264
11	1.710	0.004153	11	1.710	0.004150	11	1.710	0.004147
12	1.720	0.000000	12	1.720	0.000000	12	1.720	0.000000
13	2.020	0.000000	13	2.020	0.000000	13	2.020	0.000000
Solution36			Solution35, 34			Solution33		
1	0.000	0.126800	1	0.000	0.126800	1	0.000	0.126700
2	0.150	0.100600	2	0.150	0.100600	2	0.150	0.100600
3	0.257	0.077150	3	0.257	0.077130	3	0.257	0.077110
4	0.387	0.056380	4	0.387	0.056360	4	0.387	0.056350
5	0.557	0.038870	5	0.557	0.038870	5	0.557	0.038860
6	0.778	0.024550	6	0.778	0.024550	6	0.778	0.024540
7	1.064	0.013450	7	1.064	0.013450	7	1.064	0.013450
8	1.424	0.005816	8	1.424	0.005818	8	1.424	0.005819
9	1.868	0.001591	9	1.868	0.001593	9	1.868	0.001594
10	2.407	0.000144	10	2.407	0.000145	10	2.407	0.000145
11	3.000	0.000000	11	3.000	0.000000	11	3.000	0.000000

Solution24		Solution23, 22		Solution21				
1	0.000	0.080140	1	0.000	0.080120	1	0.000	0.080100
2	0.150	0.065140	2	0.150	0.065120	2	0.150	0.065110
3	0.257	0.051670	3	0.257	0.051660	3	0.257	0.051650
4	0.387	0.039640	4	0.387	0.039630	4	0.387	0.039630
5	0.557	0.029240	5	0.557	0.029230	5	0.557	0.029230
6	0.778	0.020330	6	0.778	0.020330	6	0.778	0.020330
7	1.064	0.012900	7	1.064	0.012900	7	1.064	0.012900
8	1.424	0.007095	8	1.424	0.007096	8	1.424	0.007096
9	1.868	0.003042	9	1.868	0.003043	9	1.868	0.003044
10	2.407	0.000743	10	2.407	0.000743	10	2.407	0.000744
11	3.000	0.000000	11	3.000	0.000000	11	3.000	0.000000
Solution24		Solution23, 22		Solution21				
1	0.000	0.080140	1	0.000	0.080120	1	0.000	0.080100
2	0.100	0.076210	2	0.100	0.076200	2	0.100	0.076190
3	0.110	0.066090	3	0.110	0.066080	3	0.110	0.066070
4	0.310	0.039350	4	0.310	0.039350	4	0.310	0.039350
5	0.510	0.029120	5	0.510	0.029120	5	0.510	0.029120
6	0.710	0.023040	6	0.710	0.023040	6	0.710	0.023040
7	0.910	0.019340	7	0.910	0.019330	7	0.910	0.019320
8	1.110	0.016790	8	1.110	0.016790	8	1.110	0.016790
9	1.310	0.014910	9	1.310	0.014910	9	1.310	0.014910
10	1.510	0.013530	10	1.510	0.013530	10	1.510	0.013530
11	1.710	0.012110	11	1.710	0.012110	11	1.710	0.012110
12	1.720	0.002213	12	1.720	0.002213	12	1.720	0.002213
13	2.020	0.001102	13	2.020	0.001101	13	2.020	0.001100
Solution20		Solution19, 18		Solution17				
1	0.000	0.049560	1	0.000	0.049540	1	0.000	0.049530
2	0.100	0.042530	2	0.100	0.042510	2	0.100	0.042510
3	0.207	0.034420	3	0.207	0.034410	3	0.207	0.034400
4	0.337	0.027530	4	0.337	0.027520	4	0.337	0.027520
5	0.507	0.021590	5	0.507	0.021580	5	0.507	0.021580
6	0.728	0.016290	6	0.728	0.016290	6	0.728	0.016290
7	1.014	0.011480	7	1.014	0.011480	7	1.014	0.011480
8	1.374	0.007184	8	1.374	0.007183	8	1.374	0.007182
9	1.819	0.003582	9	1.819	0.003582	9	1.819	0.003582
10	2.358	0.001013	10	2.358	0.001013	10	2.358	0.001013
11	3.000	0.000000	11	3.000	0.000000	11	3.000	0.000000
Solution20		Solution19, 18		Solution17				
1	0.000	0.049560	1	0.000	0.049540	1	0.000	0.049530
2	0.100	0.045730	2	0.100	0.045720	2	0.100	0.045710
3	0.110	0.035880	3	0.110	0.035870	3	0.110	0.035860
4	0.310	0.020930	4	0.310	0.020920	4	0.310	0.020920
5	0.510	0.016410	5	0.510	0.016400	5	0.510	0.016400
6	0.710	0.013500	6	0.710	0.013500	6	0.710	0.013490
7	0.910	0.012010	7	0.910	0.012000	7	0.910	0.012000
8	1.110	0.011080	8	1.110	0.011080	8	1.110	0.011070
9	1.310	0.010570	9	1.310	0.010560	9	1.310	0.010560
10	1.510	0.010280	10	1.510	0.010270	10	1.510	0.010270
11	1.710	0.010050	11	1.710	0.010050	11	1.710	0.010050
12	1.720	0.000053	12	1.720	0.000048	12	1.720	0.000046
13	2.020	0.000021	13	2.020	0.000020	13	2.020	0.000019
Solution16		Solution15, 14		Solution13				
1	0.000	0.018380	1	0.000	0.018380	1	0.000	0.018380
2	0.050	0.016400	2	0.050	0.016390	2	0.050	0.016390
3	0.159	0.014730	3	0.159	0.014730	3	0.159	0.014730
4	0.291	0.013110	4	0.291	0.013110	4	0.291	0.013110
5	0.464	0.011510	5	0.464	0.011510	5	0.464	0.011510
6	0.689	0.009744	6	0.689	0.009744	6	0.689	0.009743
7	0.980	0.007687	7	0.980	0.007687	7	0.980	0.007686
8	1.346	0.005357	8	1.346	0.005357	8	1.346	0.005357
9	1.799	0.002945	9	1.799	0.002945	9	1.799	0.002945
10	2.347	0.000897	10	2.347	0.000897	10	2.347	0.000897
11	3.000	0.000000	11	3.000	0.000000	11	3.000	0.000000

Solution16		Solution15, 14		Solution13	
1	0.000	0.018380	1	0.000	0.018380
2	0.100	0.016010	2	0.100	0.016000
3	0.110	0.006003	3	0.110	0.006000
4	0.310	0.003870	4	0.310	0.003869
5	0.510	0.002571	5	0.510	0.002570
6	0.710	0.002309	6	0.710	0.002307
7	0.910	0.001916	7	0.910	0.001915
8	1.110	0.001837	8	1.110	0.001836
9	1.310	0.001705	9	1.310	0.001704
10	1.510	0.001686	10	1.510	0.001685
11	1.710	0.001632	11	1.710	0.001631
12	1.720	0.000000	12	1.720	0.000000
13	2.020	0.000000	13	2.020	0.000000
Soluiton12		Solution11, 10		Solution9	
1	0.000	0.029370	1	0.000	0.029360
2	0.150	0.025520	2	0.150	0.025520
3	0.257	0.022030	3	0.257	0.022030
4	0.387	0.018780	4	0.387	0.018770
5	0.557	0.015660	5	0.557	0.015650
6	0.778	0.012540	6	0.778	0.012540
7	1.064	0.009375	7	1.064	0.009374
8	1.424	0.006214	8	1.424	0.006214
9	1.868	0.003270	9	1.868	0.003270
10	2.407	0.000965	10	2.407	0.000965
11	3.000	0.000000	11	3.000	0.000000
Soluiton12		Solution11, 10		Solution9	
1	0.000	0.029370	1	0.000	0.029350
2	0.100	0.028390	2	0.100	0.028380
3	0.110	0.018250	3	0.110	0.018240
4	0.310	0.011660	4	0.310	0.011650
5	0.510	0.008991	5	0.510	0.008987
6	0.710	0.007517	6	0.710	0.007513
7	0.910	0.006674	7	0.910	0.006670
8	1.110	0.006177	8	1.110	0.006174
9	1.310	0.005891	9	1.310	0.005888
10	1.510	0.005733	10	1.510	0.005730
11	1.710	0.005623	11	1.710	0.005620
12	1.720	0.000000	12	1.720	0.000000
13	2.020	0.000000	13	2.020	0.000000
Solution8		Solution7, 6		Solution5	
1	0.000	0.020020	1	0.000	0.020020
2	0.100	0.018230	2	0.100	0.018230
3	0.207	0.016130	3	0.207	0.016130
4	0.337	0.014230	4	0.337	0.014220
5	0.507	0.012330	5	0.507	0.012330
6	0.728	0.010280	6	0.728	0.010280
7	1.014	0.007998	7	1.014	0.007998
8	1.374	0.005504	8	1.374	0.005504
9	1.819	0.002993	9	1.819	0.002993
10	2.358	0.000905	10	2.358	0.000905
11	3.000	0.000000	11	3.000	0.000000
Solution8		Solution7, 6		Solution5	
1	0.000	0.020020	1	0.000	0.020010
2	0.100	0.019070	2	0.100	0.019070
3	0.110	0.008993	3	0.110	0.008987
4	0.310	0.005340	4	0.310	0.005336
5	0.510	0.004063	5	0.510	0.004060
6	0.710	0.003361	6	0.710	0.003359
7	0.910	0.002974	7	0.910	0.002972
8	1.110	0.002747	8	1.110	0.002745
9	1.310	0.002617	9	1.310	0.002615
10	1.510	0.002546	10	1.510	0.002544
11	1.710	0.002496	11	1.710	0.002494
12	1.720	0.000000	12	1.720	0.000000
13	2.020	0.000000	13	2.020	0.000000

Solution4			Solution2, 3			Solution1		
	1	0.000	0.012180		1	0.000	0.012180	
	2	0.050	0.011690		2	0.050	0.011690	
	3	0.159	0.011210		3	0.159	0.011210	
	4	0.291	0.010620		4	0.291	0.010620	
	5	0.464	0.009806		5	0.464	0.009806	
	6	0.689	0.008640		6	0.689	0.008639	
	7	0.980	0.007045		7	0.980	0.007045	
	8	1.346	0.005043		8	1.346	0.005043	
	9	1.799	0.002831		9	1.799	0.002831	
	10	2.347	0.000875		10	2.347	0.000875	
	11	3.000	0.000000		11	3.000	0.000000	
Solution4			Solution2, 3			Solution1		
	1	0.000	0.012180		1	0.000	0.012180	
	2	0.100	0.011610		2	0.100	0.011610	
	3	0.110	0.001476		3	0.110	0.001475	
	4	0.310	0.001069		4	0.310	0.001068	
	5	0.510	0.000543		5	0.510	0.000543	
	6	0.710	0.000582		6	0.710	0.000581	
	7	0.910	0.000425		7	0.910	0.000425	
	8	1.110	0.000441		8	1.110	0.000441	
	9	1.310	0.000389		9	1.310	0.000388	
	10	1.510	0.000398		10	1.510	0.000397	
	11	1.710	0.000375		11	1.710	0.000374	
	12	1.720	0.000000		12	1.720	0.000000	
	13	2.020	0.000000		13	2.020	0.000000	

86	1.5	0.920	0.809	0.00590	0.30	0.44	83.5	96.5	0.00	0.00
87	1.5	0.920	0.811	0.00590	0.30	0.44	83.4	96.6	0.00	0.00
89	1.5	0.920	0.808	0.00590	0.30	0.44	83.5	96.5	0.00	0.00
90	1.5	0.919	0.810	0.00590	0.30	0.44	83.5	96.6	0.00	0.00
85	1.5	0.921	0.810	0.00590	0.30	0.44	83.6	96.5	0.00	0.00
88	1.5	0.920	0.811	0.00590	0.30	0.44	83.5	96.5	0.00	0.00
91	1.5	0.922	0.810	0.00590	0.30	0.44	83.6	96.5	0.00	0.00

APPENDIX C

I-DEAS LIST FILE OF THE PRESSURE AT 100MPA AND 0.3MM DIAMETER NOZZLE.

I-DEAS Master Series 5: Model Solution Nonlinear Solver
29-Apr-99 15:44:14 PAGE 1

MODEL_SOLUTION_SOLVE

MODEL FILE : /scratch/jay/i/tef100.mf1

MODEL FILE DESCRIPTION : /scratch/jay/i/tef100.mf1

FE MODEL : skin

PART : skin

NUMBER OF NODES : 1053

NUMBER OF ELEMENTS : 700

ACTIVE UNITS SYSTEM : mm (milli-newton)

TEMPERATURE MODE : Relative Temperatures

SOLUTION SET 1 : SOLUTION SET1

TIME = 0.0000 BOUNDARY SET : P100000

RESTRAINT SET : RESTRAINT SET 1

CONTACT SET : CONTACT SET 1

LOAD SET 9 : P40000

15:44:15 (CP 0.46 0.46) NON-LINEAR STATIC ANALYSIS

15:44:18 (CP 3.29 3.75) Offset Tables Formed

15:44:19 (CP 0.22 3.97)

15:44:19 (CP 0.03 4.00) Next Solution Point: 1

15:44:19 (CP 0.02 4.02)

15:44:19 (CP 0.04 4.06)

15:44:19 (CP 0.02 4.08) Current Time: 1

15:44:19 (CP 0.01 4.09)

I-DEAS Master Series 5: Model Solution Nonlinear Solver
29-Apr-99 15:44:20 PAGE 2

MODEL_SOLUTION_SOLVE

THIS CONSTRAINT USE ORTHOTROPIC MATERIALS.

15:44:21 (CP 1.93 6.02) Material Tables Formed

15:44:22 (CP 1.00 7.02) Begin Constraint Partitioning

15:44:28 (CP 4.97 11.99)

15:44:28 (CP 0.01 12.00) Equilibrium Iteration Number: 1

15:44:28 (CP 0.01 12.01)

15:44:28 (CP 0.03 12.04) ----- Begin Iteration -----

15:44:32 (CP 3.07 15.11) Number of potential contact elements : 690

15:44:32 (CP 0.16 15.27) Contact Element Offsets Formed

15:44:35 (CP 1.28 16.55) Contact Stiffness Matrix Formation Complete

15:44:35 (CP 0.05 16.60) Form Contact Status

15:44:35 (CP 0.27 16.87) Number of contact status changes: 0

15:44:36 (CP 0.02 16.89) Number of inactive contacts: 0

15:44:36 (CP 0.01 16.90) Number of active open contacts: 140

15:44:36 (CP 0.03 16.93) Number of sticking contacts: 0

15:44:36 (CP 0.03 16.96) Number of sliding contacts: 0

15:44:36 (CP 0.63 17.59) Begin Stiffness Matrix Formation

15:44:46 (CP 7.05 24.64) Begin External Loads Formation

15:44:47 (CP 0.78 25.42) External Loads Formation Complete

15:44:47 (CP 0.10 25.52) Begin Internal Force Formation

15:44:50 (CP 2.47 27.99) Internal Force Formation Complete

15:44:50 (CP 0.25 28.24) Begin Stiffness Matrix Partitioning

15:44:57 (CP 3.53 31.77) Contact Stiffness Partitions Formed
 15:44:57 (CP 0.01 31.78) Stiffness Matrix Formation Complete
 TOTAL VIRTUAL MEMORY SPECIFIED = 185 MB
 PERCENT ALLOCATED TO APPLICATION MEMORY = 64 %
 MEMORY ALLOCATED FOR SPARSE MATRIX SOLVER = 29 MB
 MEMORY USED BY SPARSE MATRIX SOLVER = 7 MB
 15:44:59 (CP 1.93 33.71) Sparse solve will be done in-memory
 15:44:59 (CP 0.63 34.34) Est. decomp time = 11 cpu seconds
 15:45:00 (CP 0.30 34.64) Begin Decomposition
 SIZE OF SCRATCH FILES = 1 MB

CHOLESKY DECOMPOSITION STATISTICS:

SINGULARITY CRITERIA = 1.0E-14

NUMBER OF EQUATIONS = 2587

MINIMUM			MAXIMUM		
CHOLESKY EQUATION	NODE AND		CHOLESKY EQUATION	NODE AND	
PIVOTS	NUMBER	DIRECTION	PIVOTS	NUMBER	DIRECTION

1.3187D+03	796	370-Y	3.2453D+06	16	22-Y
1.7419D+03	774	338-Y	3.1965D+06	982	510-Y
2.1869D+03	727	321-Y	1.9835D+06	19	23-Y
2.3136D+03	793	345-Y	1.7098D+06	4	18-Y
2.5392D+03	749	329-Y	1.6691D+06	60	38-Y

I-DEAS Master Series 5: Model Solution Nonlinear Solver

29-Apr-99 15:45:07 PAGE 3

MODEL SOLUTION SOLVE

2.5456D+03	730	322-Y	1.6228D+06	2	17-Y
2.6562D+03	750	329-Z	1.6225D+06	21	24-Y
3.0101D+03	728	321-Z	1.5424D+06	13	21-Y
3.0131D+03	664	298-Y	1.4431D+06	38	30-Y
3.0472D+03	776	339-Y	1.4405D+06	32	28-Y
3.2105D+03	685	306-X	1.3574D+06	29	27-Y
3.2467D+03	683	305-Y	1.2895D+06	1378	654-Y
3.2696D+03	708	314-Y	1.1819D+06	26	26-Y
3.3198D+03	788	343-Y	1.1455D+06	63	39-Y
3.3331D+03	706	313-Z	1.0751D+06	7	19-Y
3.4636D+03	785	342-Y	9.4981D+05	48	34-Y
3.4877D+03	639	289-Y	8.9130D+05	73	43-Y
3.5414D+03	779	340-Y	8.8663D+05	82	46-Y
3.5470D+03	795	354-Y	8.8376D+05	51	35-Y
3.5677D+03	729	322-X	8.5380D+05	104	54-Y

15:45:08 (CP 7.12 41.76) End Of Decomposition
 15:45:08 (CP 0.21 41.97) Begin Contact Force Iteration
 15:45:15 (CP 4.97 46.94) ----- End of Iteration -----
 15:45:15 (CP 0.02 46.96)
 15:45:16 (CP 0.92 47.88) Stiffness Parameter for Iteration : 1
 15:45:17 (CP 1.33 49.21)
 15:45:18 (CP 0.02 49.23) Equilibrium Iteration Number: 2
 15:45:18 (CP 0.03 49.26)
 15:45:18 (CP 0.02 49.28) ----- Begin Iteration -----
 15:45:18 (CP 0.15 49.43) Form Contact Status
 15:45:18 (CP 0.35 49.78) Number of contact status changes: 140
 15:45:18 (CP 0.04 49.82) Number of inactive contacts: 63

15:45:19 (CP 0.02 49.84) Number of active open contacts: 0
 15:45:19 (CP 0.03 49.87) Number of sticking contacts: 77
 15:45:19 (CP 0.01 49.88) Number of sliding contacts: 0
 15:45:19 (CP 0.61 50.49) Begin Stiffness Matrix Formation
 15:45:28 (CP 6.44 56.93) Begin External Loads Formation
 15:45:29 (CP 0.68 57.61) External Loads Formation Complete
 15:45:29 (CP 0.42 58.03) Begin Internal Force Formation
 15:45:33 (CP 2.62 60.65) Internal Force Formation Complete
 15:45:33 (CP 0.03 60.68) Begin Stress Stiffness Matrix Formation
 15:45:39 (CP 2.31 62.99) Begin Stiffness Matrix Partitioning
 15:45:45 (CP 3.20 66.19) Contact Stiffness Partitions Formed
 15:45:45 (CP 0.03 66.22) Stiffness Matrix Formation Complete
 TOTAL VIRTUAL MEMORY SPECIFIED = 185 MB
 PERCENT ALLOCATED TO APPLICATION MEMORY = 64 %
 MEMORY ALLOCATED FOR SPARSE MATRIX SOLVER = 29 MB
 MEMORY USED BY SPARSE MATRIX SOLVER = 7 MB
 15:45:47 (CP 1.78 68.00) Sparse solve will be done in-memory
 15:45:48 (CP 0.63 68.63) Est. decomp time = 12 cpu seconds
 15:45:48 (CP 0.11 68.74) Begin Decomposition
 SIZE OF SCRATCH FILES = 1 MB

CHOLESKY DECOMPOSITION STATISTICS:

SINGULARITY CRITERIA = 1.0E-14
 NUMBER OF EQUATIONS = 2587

MINIMUM			MAXIMUM		
CHOLESKY EQUATION	NODE AND	PIVOTS	CHOLESKY EQUATION	NODE AND	PIVOTS
NUMBER	DIRECTION		NUMBER	DIRECTION	

1.6551D+03	774	338-Y	1.6472D+06	7	19-Y
1.6792D+03	796	370-Y	1.5235D+06	13	21-Y

I-DEAS Master Series 5: Model Solution Nonlinear Solver

29-Apr-99 15:45:56 PAGE 4

MODEL_SOLUTION_SOLVE

1.6910D+03	793	345-Y	1.4429D+06	38	30-Y
1.7967D+03	749	329-Y	1.4402D+06	32	28-Y
2.0403D+03	730	322-Y	1.3583D+06	16	22-Y
2.1374D+03	727	321-Y	1.3546D+06	10	20-Y
2.1627D+03	795	354-Y	1.2728D+06	26	26-Y
2.9931D+03	639	289-Y	1.1849D+06	41	31-Y
2.9998D+03	782	341-Y	9.7320D+05	54	36-Y
3.0520D+03	708	314-Y	8.9656D+05	60	38-Y
3.0868D+03	750	329-Z	8.6151D+05	48	34-Y
3.0943D+03	728	321-Z	8.4608D+05	63	39-Y
3.1655D+03	620	282-Y	8.2996D+05	104	54-Y
3.1860D+03	2587	1227-Y	8.2441D+05	51	35-Y
3.2014D+03	788	343-Y	8.1785D+05	57	37-Y
3.2382D+03	785	342-Y	7.8704D+05	4	18-Y
3.2547D+03	779	340-Y	7.2212D+05	43	32-Y
3.2609D+03	791	344-Y	7.2150D+05	24	25-Y
3.2755D+03	683	305-Y	6.7978D+05	2	17-Y
3.2883D+03	664	298-Y	6.7914D+05	21	24-Y
15:45:56 (CP 7.63	76.37)	End Of Decomposition			
15:45:56 (CP 0.13	76.50)	Begin Contact Force Iteration			

15:46:37 (CP 30.58 107.08) Contact force convergence ratio: 0.012928
 15:46:38 (CP 0.18 107.26) ----- End of Iteration -----
 15:46:38 (CP 0.01 107.27)
 15:46:39 (CP 0.94 108.21) Stiffness Parameter for Iteration : 0.009582518
 15:46:40 (CP 0.41 108.62) Convergence Statistics
 15:46:41 (CP 0.63 109.25) Energy Convergence Ratio: 0.04322678
 15:46:41 (CP 0.19 109.44)
 15:46:41 (CP 0.02 109.46) Equilibrium Iteration Number: 3
 15:46:41 (CP 0.02 109.48)
 15:46:41 (CP 0.01 109.49) ----- Begin Iteration -----
 15:46:42 (CP 0.16 109.65) Form Contact Status
 15:46:42 (CP 0.39 110.04) Number of contact status changes: 112
 15:46:42 (CP 0.04 110.08) Number of inactive contacts: 52
 15:46:42 (CP 0.03 110.11) Number of active open contacts: 0
 15:46:43 (CP 0.01 110.12) Number of sticking contacts: 35
 15:46:43 (CP 0.02 110.14) Number of sliding contacts: 53
 15:46:43 (CP 0.67 110.81) Begin Stiffness Matrix Formation
 15:46:54 (CP 6.48 117.29) Begin External Loads Formation
 15:46:56 (CP 0.76 118.05) External Loads Formation Complete
 15:46:58 (CP 0.40 118.45) Begin Internal Force Formation
 15:47:02 (CP 2.57 121.02) Internal Force Formation Complete
 15:47:02 (CP 0.05 121.07) Begin Stress Stiffness Matrix Formation
 15:47:08 (CP 2.26 123.33) Begin Stiffness Matrix Partitioning
 15:47:13 (CP 3.17 126.50) Contact Stiffness Partitions Formed
 15:47:13 (CP 0.02 126.52) Stiffness Matrix Formation Complete
 TOTAL VIRTUAL MEMORY SPECIFIED = 185 MB
 PERCENT ALLOCATED TO APPLICATION MEMORY = 64 %
 MEMORY ALLOCATED FOR SPARSE MATRIX SOLVER = 29 MB
 MEMORY USED BY SPARSE MATRIX SOLVER = 7 MB
 15:47:16 (CP 1.84 128.36) Sparse solve will be done in-memory
 15:47:16 (CP 0.60 128.96) Est. decomp time = 11 cpu seconds
 15:47:17 (CP 0.10 129.06) Begin Decomposition
 SIZE OF SCRATCH FILES = 1 MB

CHOLESKY DECOMPOSITION STATISTICS:
 SINGULARITY CRITERIA = 1.0E-14
 NUMBER OF EQUATIONS = 2587

MINIMUM		MAXIMUM			
CHOLESKY EQUATION	NODE AND	CHOLESKY EQUATION	NODE AND		
PIVOTS	NUMBER DIRECTION	PIVOTS	NUMBER DIRECTION		

I-DEAS Master Series 5: Model Solution Nonlinear Solver

29-Apr-99 15:47:24 PAGE 5

MODEL_SOLUTION_SOLVE

1.3093D+03	796	370-Y	1.3402D+06	13	21-Y
1.8025D+03	774	338-Y	1.3321D+06	16	22-Y
1.8040D+03	727	321-Y	1.3309D+06	7	19-Y
2.3325D+03	793	345-Y	1.2653D+06	4	18-Y
2.8539D+03	639	289-Y	1.2619D+06	19	23-Y
3.0703D+03	730	322-Y	1.2446D+06	60	38-Y
3.1126D+03	664	298-Y	1.2313D+06	10	20-Y
3.2826D+03	683	305-Y	9.8423D+05	48	34-Y
3.3107D+03	708	314-Y	9.5580D+05	54	36-Y
3.3210D+03	776	339-Y	9.3295D+05	63	39-Y
3.3422D+03	795	354-Y	8.8586D+05	57	37-Y

```

3.3843D+03 728 321-Z      8.8282D+05 73 43-Y
3.4502D+03 782 341-Y      8.8008D+05 79 45-Y
3.4966D+03 779 340-Y      8.7888D+05 51 35-Y
3.5197D+03 729 322-X      8.2302D+05 107 55-Y
3.5284D+03 788 343-Y      7.7645D+05 95 51-Y
3.5424D+03 620 282-Y      7.2245D+05 2 17-Y
3.5799D+03 725 320-Y      7.2232D+05 21 24-Y
3.6449D+03 685 306-X      6.9641D+05 90 49-Y
3.6925D+03 663 298-X      6.9583D+05 101 53-Y
15:47:24 (CP 7.11 136.17) End Of Decomposition
15:47:24 (CP 0.10 136.27) Begin Contact Force Iteration
15:50:22 (CP 141.19 277.46) Contact force convergence ratio: 0.01499246
15:50:23 (CP 0.21 277.67) ----- End of Iteration -----
15:50:23 (CP 0.03 277.70)
15:50:24 (CP 0.99 278.69) Stiffness Parameter for Iteration : 0.0123823
15:50:24 (CP 0.41 279.10) Convergence Statistics
15:50:25 (CP 0.62 279.72) Energy Convergence Ratio: 0.11055
15:50:25 (CP 0.21 279.93)
15:50:25 (CP 0.02 279.95) Equilibrium Iteration Number: 4
15:50:26 (CP 0.02 279.97)
15:50:26 (CP 0.02 279.99) ----- Begin Iteration -----
15:50:26 (CP 0.15 280.14) Form Contact Status
15:50:26 (CP 0.38 280.52) Number of contact status changes: 83
15:50:26 (CP 0.03 280.55) Number of inactive contacts: 73
15:50:27 (CP 0.02 280.57) Number of active open contacts: 0
15:50:27 (CP 0.01 280.58) Number of sticking contacts: 36
15:50:27 (CP 0.02 280.60) Number of sliding contacts: 31
15:50:28 (CP 0.66 281.26) Begin Stiffness Matrix Formation
15:50:37 (CP 6.32 287.58) Begin External Loads Formation
15:50:38 (CP 0.59 288.17) External Loads Formation Complete
15:50:39 (CP 0.42 288.59) Begin Internal Force Formation
15:50:42 (CP 2.48 291.07) Internal Force Formation Complete
15:50:42 (CP 0.04 291.11) Begin Stress Stiffness Matrix Formation
15:50:47 (CP 2.18 293.29) Begin Stiffness Matrix Partitioning
15:50:52 (CP 2.88 296.17) Contact Stiffness Partitions Formed
15:50:52 (CP 0.04 296.21) Stiffness Matrix Formation Complete
TOTAL VIRTUAL MEMORY SPECIFIED = 185 MB
PERCENT ALLOCATED TO APPLICATION MEMORY = 64 %
MEMORY ALLOCATED FOR SPARSE MATRIX SOLVER = 29 MB
MEMORY USED BY SPARSE MATRIX SOLVER = 7 MB
15:50:54 (CP 1.75 297.96) Sparse solve will be done in-memory
15:50:55 (CP 0.62 298.58) Est. decomp time = 12 cpu seconds
15:50:55 (CP 0.08 298.66) Begin Decomposition
SIZE OF SCRATCH FILES = 1 MB

```

CHOLESKY DECOMPOSITION STATISTICS:

SINGULARITY CRITERIA = 1.0E-14
NUMBER OF EQUATIONS = 2587

I-DEAS Master Series 5: Model Solution Nonlinear Solver
29-Apr-99 15:51:03 PAGE 6
MODEL_SOLUTION_SOLVE

MINIMUM MAXIMUM
CHOLESKY EQUATION NODE AND CHOLESKY EQUATION NODE AND
PIVOTS NUMBER DIRECTION PIVOTS NUMBER DIRECTION

1.3088D+03	796	370-Y	1.3402D+06	13	21-Y
1.8048D+03	774	338-Y	1.3321D+06	16	22-Y
2.3203D+03	793	345-Y	1.3309D+06	7	19-Y
2.5496D+03	727	321-Y	1.2653D+06	4	18-Y
2.5768D+03	766	335-Y	1.2619D+06	19	23-Y
2.7336D+03	749	329-Y	1.2310D+06	10	20-Y
2.7413D+03	639	289-Y	1.1672D+06	60	38-Y
3.0156D+03	664	298-Y	9.9727D+05	54	36-Y
3.0494D+03	485	233-Y	9.6137D+05	48	34-Y
3.0672D+03	730	322-Y	8.8584D+05	57	37-Y
3.2426D+03	795	354-Y	8.8284D+05	73	43-Y
3.2721D+03	683	305-Y	8.8010D+05	79	45-Y
3.2990D+03	708	314-Y	8.7885D+05	51	35-Y
3.3959D+03	776	339-Y	7.2710D+05	63	39-Y
3.4002D+03	782	341-Y	7.2243D+05	2	17-Y
3.4014D+03	750	329-Z	7.2230D+05	21	24-Y
3.4208D+03	685	306-X	5.8072D+05	107	55-Y
3.4225D+03	722	319-Y	5.4752D+05	95	51-Y
3.4475D+03	686	306-Y	5.4237D+05	129	63-Y
3.4737D+03	640	289-Z	5.4047D+05	104	54-Y
15:51:03 (CP	7.42	306.08) End Of Decomposition			
15:51:03 (CP	0.11	306.19) Begin Contact Force Iteration			
15:51:25 (CP	17.04	323.23) Contact force convergence ratio: 0.003797837			
15:51:25 (CP	0.18	323.41) ----- End of Iteration -----			
15:51:25 (CP	0.01	323.42)			
15:51:26 (CP	0.99	324.41) Stiffness Parameter for Iteration : 0.01062391			
15:51:27 (CP	0.41	324.82) Convergence Statistics			
15:51:27 (CP	0.62	325.44) Energy Convergence Ratio: 0.03658985			
15:51:28 (CP	0.20	325.64)			
15:51:28 (CP	0.02	325.66) Equilibrium Iteration Number: 5			
15:51:28 (CP	0.03	325.69)			
15:51:28 (CP	0.02	325.71) ----- Begin Iteration -----			
15:51:28 (CP	0.17	325.88) Form Contact Status			
15:51:29 (CP	0.35	326.23) Number of contact status changes: 68			
15:51:29 (CP	0.03	326.26) Number of inactive contacts: 75			
15:51:29 (CP	0.02	326.28) Number of active open contacts: 0			
15:51:29 (CP	0.02	326.30) Number of sticking contacts: 25			
15:51:29 (CP	0.02	326.32) Number of sliding contacts: 40			
15:51:31 (CP	0.63	326.95) Begin Stiffness Matrix Formation			
15:51:39 (CP	6.38	333.33) Begin External Loads Formation			
15:51:40 (CP	0.59	333.92) External Loads Formation Complete			
15:51:41 (CP	0.36	334.28) Begin Internal Force Formation			
15:51:44 (CP	2.53	336.81) Internal Force Formation Complete			
15:51:44 (CP	0.03	336.84) Begin Stress Stiffness Matrix Formation			
15:51:49 (CP	2.16	339.00) Begin Stiffness Matrix Partitioning			
15:51:54 (CP	2.86	341.86) Contact Stiffness Partitions Formed			
15:51:55 (CP	0.03	341.89) Stiffness Matrix Formation Complete			

I-DEAS Master Series 5: Model Solution Nonlinear Solver

29-Apr-99 15:51:55 PAGE 7

MODEL_SOLUTION_SOLVE

TOTAL VIRTUAL MEMORY SPECIFIED = 185 MB

PERCENT ALLOCATED TO APPLICATION MEMORY = 64 %

MEMORY ALLOCATED FOR SPARSE MATRIX SOLVER = 29 MB

MEMORY USED BY SPARSE MATRIX SOLVER = 7 MB
 15:51:57 (CP 1.79 343.68) Sparse solve will be done in-memory
 15:51:57 (CP 0.62 344.30) Est. decomp time = 10 cpu seconds
 15:51:58 (CP 0.11 344.41) Begin Decomposition
 SIZE OF SCRATCH FILES = 1 MB

CHOLESKY DECOMPOSITION STATISTICS:
 SINGULARITY CRITERIA = 1.0E-14
 NUMBER OF EQUATIONS = 2587

MINIMUM		MAXIMUM			
CHOLESKY EQUATION	NODE AND	CHOLESKY EQUATION	NODE AND		
PIVOTS	NUMBER DIRECTION	PIVOTS	NUMBER DIRECTION		

1.6286D+03	796	370-Y	1.3401D+06	13	21-Y
1.7378D+03	793	345-Y	1.3321D+06	16	22-Y
1.7422D+03	749	329-Y	1.3308D+06	7	19-Y
1.7931D+03	795	354-Y	1.2652D+06	4	18-Y
2.0910D+03	774	338-Y	1.2619D+06	19	23-Y
2.1879D+03	730	322-Y	1.2287D+06	10	20-Y
2.3128D+03	485	233-Y	8.8509D+05	57	37-Y
2.5224D+03	727	321-Y	8.7769D+05	51	35-Y
2.5383D+03	788	343-Y	8.1083D+05	60	38-Y
2.7432D+03	586	306-Y	7.4178D+05	54	36-Y
2.9885D+03	639	289-Y	7.2342D+05	48	34-Y
3.0329D+03	664	298-Y	7.2241D+05	2	17-Y
3.0491D+03	782	341-Y	7.2227D+05	21	24-Y
3.1174D+03	728	321-Z	7.0512D+05	98	52-Y
3.2016D+03	685	306-X	6.8704D+05	63	39-Y
3.2812D+03	683	305-Y	5.4178D+05	129	63-Y
3.3087D+03	708	314-Y	5.2825D+05	123	61-Y
3.3259D+03	766	335-Y	5.2632D+05	126	62-Y
3.3577D+03	779	340-Y	5.2390D+05	6	19-X
3.3590D+03	791	344-Y	5.2308D+05	117	59-Y
15:52:04 (CP	6.29	350.70)	End Of Decomposition		
15:52:04 (CP	0.12	350.82)	Begin Contact Force Iteration		
15:52:25 (CP	16.99	367.81)	Contact force convergence ratio: 0.01164932		
15:52:26 (CP	0.20	368.01)	----- End of Iteration -----		
15:52:26 (CP	0.03	368.04)			
15:52:27 (CP	1.01	369.05)	Stiffness Parameter for Iteration : 0.01092882		
15:52:27 (CP	0.40	369.45)	Convergence Statistics		
15:52:28 (CP	0.61	370.06)	Energy Convergence Ratio: 0.006853286		
15:52:28 (CP	0.18	370.24)			
15:52:28 (CP	0.03	370.27)	Equilibrium Iteration Number: 6		
15:52:29 (CP	0.02	370.29)			
15:52:29 (CP	0.01	370.30)	----- Begin Iteration -----		
15:52:29 (CP	0.19	370.49)	Form Contact Status		
15:52:29 (CP	0.37	370.86)	Number of contact status changes: 35		
15:52:29 (CP	0.03	370.89)	Number of inactive contacts: 79		
15:52:29 (CP	0.02	370.91)	Number of active open contacts: 0		
15:52:30 (CP	0.01	370.92)	Number of sticking contacts: 10		
15:52:30 (CP	0.03	370.95)	Number of sliding contacts: 51		
15:52:32 (CP	0.77	371.72)	Begin Stiffness Matrix Formation		
15:52:41 (CP	6.38	378.10)	Begin External Loads Formation		
15:52:41 (CP	0.62	378.72)	External Loads Formation Complete		

I-DEAS Master Series 5: Model Solution Nonlinear Solver

29-Apr-99 15:52:41 PAGE 8

MODEL_SOLUTION_SOLVE

15:52:42 (CP 0.40 379.12) Begin Internal Force Formation
 15:52:45 (CP 2.46 381.58) Internal Force Formation Complete
 15:52:46 (CP 0.05 381.63) Begin Stress Stiffness Matrix Formation
 15:52:51 (CP 2.16 383.79) Begin Stiffness Matrix Partitioning
 15:52:55 (CP 2.73 386.52) Contact Stiffness Partitions Formed
 15:52:55 (CP 0.03 386.55) Stiffness Matrix Formation Complete
 TOTAL VIRTUAL MEMORY SPECIFIED = 185 MB
 PERCENT ALLOCATED TO APPLICATION MEMORY = 64 %
 MEMORY ALLOCATED FOR SPARSE MATRIX SOLVER = 29 MB
 MEMORY USED BY SPARSE MATRIX SOLVER = 6 MB
 15:52:58 (CP 1.69 388.24) Sparse solve will be done in-memory
 15:52:58 (CP 0.62 388.86) Est. decomp time = 9 cpu seconds
 15:52:58 (CP 0.10 388.96) Begin Decomposition
 SIZE OF SCRATCH FILES = 1 MB

CHOLESKY DECOMPOSITION STATISTICS:

SINGULARITY CRITERIA = 1.0E-14

NUMBER OF EQUATIONS = 2587

MINIMUM			MAXIMUM		
CHOLESKY EQUATION PIVOTS	NUMBER	DIRECTION	CHOLESKY EQUATION PIVOTS	NUMBER	DIRECTION

1.3080D+03	796	370-Y	1.3401D+06	13	21-Y
1.7488D+03	774	338-Y	1.3321D+06	16	22-Y
1.9464D+03	485	233-Y	1.3308D+06	7	19-Y
2.3507D+03	793	345-Y	1.2652D+06	4	18-Y
2.3602D+03	727	321-Y	1.2619D+06	19	23-Y
2.5994D+03	749	329-Y	1.2285D+06	10	20-Y
2.8084D+03	175	80-Y	8.1493D+05	57	37-Y
2.8675D+03	730	322-Y	8.0538D+05	60	38-Y
3.0466D+03	664	298-Y	7.9978D+05	51	35-Y
3.1448D+03	795	354-Y	7.4101D+05	54	36-Y
3.1805D+03	788	343-Y	7.3387D+05	48	34-Y
3.2306D+03	782	341-Y	7.3110D+05	63	39-Y
3.2681D+03	750	329-Z	7.2240D+05	2	17-Y
3.2887D+03	683	305-Y	7.2227D+05	21	24-Y
3.3082D+03	785	342-Y	5.3266D+05	92	50-Y
3.3190D+03	708	314-Y	5.2639D+05	107	55-Y
3.3348D+03	776	339-Y	5.2389D+05	6	19-X
3.3544D+03	728	321-Z	5.2109D+05	17	22-Z
3.3738D+03	618	281-Z	5.2015D+05	3	18-X
3.4054D+03	706	313-Z	5.1870D+05	20	23-Z
15:53:04 (CP 5.42	394.38)	End Of Decomposition			
15:53:04 (CP 0.11	394.49)	Begin Contact Force Iteration			
15:53:33 (CP 23.41	417.90)	Contact force convergence ratio: 0.00749641			
15:53:33 (CP 0.19	418.09)	----- End of Iteration -----			
15:53:33 (CP 0.02	418.11)				
15:53:34 (CP 1.02	419.13)	Stiffness Parameter for Iteration : 0.01063938			
15:53:35 (CP 0.42	419.55)	Convergence Statistics			
15:53:36 (CP 0.62	420.17)	Energy Convergence Ratio: 0.02109787			

15:53:36 (CP 0.19 420.36)
 15:53:36 (CP 0.01 420.37) Equilibrium Iteration Number: 7
 15:53:36 (CP 0.03 420.40)
 15:53:36 (CP 0.02 420.42) ----- Begin Iteration -----
 15:53:36 (CP 0.17 420.59) Form Contact Status
 15:53:37 (CP 0.35 420.94) Number of contact status changes: 25
 15:53:37 (CP 0.03 420.97) Number of inactive contacts: 92

I-DEAS Master Series 5: Model Solution Nonlinear Solver
 29-Apr-99 15:53:37 PAGE 9

MODEL_SOLUTION_SOLVE

15:53:37 (CP 0.06 421.03) Number of active open contacts: 0
 15:53:37 (CP 0.03 421.06) Number of sticking contacts: 2
 15:53:37 (CP 0.03 421.09) Number of sliding contacts: 46
 15:53:39 (CP 0.68 421.77) Begin Stiffness Matrix Formation
 15:53:48 (CP 6.35 428.12) Begin External Loads Formation
 15:53:49 (CP 0.67 428.79) External Loads Formation Complete
 15:53:50 (CP 0.37 429.16) Begin Internal Force Formation
 15:53:53 (CP 2.49 431.65) Internal Force Formation Complete
 15:53:53 (CP 0.04 431.69) Begin Stress Stiffness Matrix Formation
 15:53:57 (CP 2.21 433.90) Begin Stiffness Matrix Partitioning
 15:54:02 (CP 2.58 436.48) Contact Stiffness Partitions Formed
 15:54:02 (CP 0.03 436.51) Stiffness Matrix Formation Complete

TOTAL VIRTUAL MEMORY SPECIFIED = 185 MB

PERCENT ALLOCATED TO APPLICATION MEMORY = 64 %

MEMORY ALLOCATED FOR SPARSE MATRIX SOLVER = 29 MB

MEMORY USED BY SPARSE MATRIX SOLVER = 6 MB

15:54:04 (CP 1.66 438.17) Sparse solve will be done in-memory

15:54:04 (CP 0.62 438.79) Est. decomp time = 7 cpu seconds

15:54:05 (CP 0.09 438.88) Begin Decomposition

SIZE OF SCRATCH FILES = 1 MB

CHOLESKY DECOMPOSITION STATISTICS:

SINGULARITY CRITERIA = 1.0E-14

NUMBER OF EQUATIONS = 2587

MINIMUM			MAXIMUM		
CHOLESKY EQUATION	NODE AND		CHOLESKY EQUATION	NODE AND	
PIVOTS	NUMBER	DIRECTION	PIVOTS	NUMBER	DIRECTION

1.2964D+03	796	370-Y	1.3401D+06	13	21-Y
1.8005D+03	774	338-Y	1.3320D+06	16	22-Y
2.3145D+03	485	233-Y	1.3308D+06	7	19-Y
2.3155D+03	793	345-Y	1.2652D+06	4	18-Y
2.5466D+03	727	321-Y	1.2618D+06	19	23-Y
2.5688D+03	766	335-Y	1.2305D+06	10	20-Y
2.7017D+03	639	289-Y	8.8503D+05	57	37-Y
2.7285D+03	749	329-Y	8.7763D+05	51	35-Y
2.8197D+03	573	265-Y	8.1049D+05	60	38-Y
3.0166D+03	664	298-Y	7.4085D+05	54	36-Y
3.0631D+03	730	322-Y	7.2247D+05	48	34-Y
3.0994D+03	87	48-Y	7.2240D+05	2	17-Y
3.1430D+03	750	329-Z	7.2226D+05	21	24-Y
3.1837D+03	685	306-X	6.8060D+05	63	39-Y
3.2093D+03	640	289-Z	5.2474D+05	101	53-Y

3.2300D+03 795 354-Y 5.2388D+05 6 19-X
 3.2702D+03 683 305-Y 5.2112D+05 107 55-Y
 3.2970D+03 708 314-Y 5.2107D+05 17 22-Z
 3.3867D+03 776 339-Y 5.2013D+05 3 18-X
 3.3944D+03 782 341-Y 5.1868D+05 20 23-Z
 15:54:10 (CP 4.53 443.41) End Of Decomposition
 15:54:10 (CP 0.13 443.54) Begin Contact Force Iteration
 15:54:31 (CP 16.86 460.40) Contact force convergence ratio: 0.005358884
 15:54:31 (CP 0.16 460.56) ----- End of Iteration -----
 15:54:31 (CP 0.02 460.58)
 15:54:32 (CP 0.98 461.56) Stiffness Parameter for Iteration : 0.01068372
 15:54:33 (CP 0.42 461.98) Convergence Statistics
 15:54:34 (CP 0.60 462.58) Energy Convergence Ratio. 0.000861518
 15:54:34 (CP 0.19 462.77)

I-DEAS Master Series 5: Model Solution Nonlinear Solver
 29-Apr-99 15:54:34 PAGE 10

MODEL_SOLUTION_SOLVE

15:54:34 (CP 0.05 462.82) Equilibrium Iteration Number: 8
 15:54:34 (CP 0.02 462.84)
 15:54:34 (CP 0.03 462.87) ----- Begin Iteration -----
 15:54:34 (CP 0.17 463.04) Form Contact Status
 15:54:35 (CP 0.37 463.41) Number of contact status changes: 3
 15:54:35 (CP 0.03 463.44) Number of inactive contacts: 91
 15:54:35 (CP 0.01 463.45) Number of active open contacts: 0
 15:54:35 (CP 0.02 463.47) Number of sticking contacts: 1
 15:54:35 (CP 0.02 463.49) Number of sliding contacts: 48
 15:54:37 (CP 0.77 464.26) Begin Stiffness Matrix Formation
 15:54:46 (CP 6.33 470.59) Begin External Loads Formation
 15:54:47 (CP 0.69 471.28) External Loads Formation Complete
 15:54:48 (CP 0.29 471.57) Begin Internal Force Formation
 15:54:51 (CP 2.50 474.07) Internal Force Formation Complete
 15:54:51 (CP 0.03 474.10) Begin Stress Stiffness Matrix Formation
 15:54:56 (CP 2.18 476.28) Begin Stiffness Matrix Partitioning
 15:55:01 (CP 2.75 479.03) Contact Stiffness Partitions Formed
 15:55:01 (CP 0.01 479.04) Stiffness Matrix Formation Complete
 TOTAL VIRTUAL MEMORY SPECIFIED = 185 MB
 PERCENT ALLOCATED TO APPLICATION MEMORY = 64 %
 MEMORY ALLOCATED FOR SPARSE MATRIX SOLVER = 29 MB
 MEMORY USED BY SPARSE MATRIX SOLVER = 6 MB
 15:55:04 (CP 1.73 480.77) Sparse solve will be done in-memory
 15:55:05 (CP 0.61 481.38) Est. decomp time = 7 cpu seconds
 15:55:05 (CP 0.09 481.47) Begin Decomposition
 SIZE OF SCRATCH FILES = 1 MB

CHOLESKY DECOMPOSITION STATISTICS:

SINGULARITY CRITERIA = 1.0E-14
 NUMBER OF EQUATIONS = 2587

MINIMUM MAXIMUM
 CHOLESKY EQUATION NODE AND CHOLESKY EQUATION NODE AND
 PIVOTS NUMBER DIRECTION PIVOTS NUMBER DIRECTION

1.2981D+03 796 370-Y 1.3401D+06 13 21-Y
 1.7908D+03 774 338-Y 1.3320D+06 16 22-Y

2.3055D+03	793	345-Y	1.3308D+06	7	19-Y
2.3146D+03	485	233-Y	1.2652D+06	4	18-Y
2.5450D+03	727	321-Y	1.2618D+06	19	23-Y
2.5571D+03	766	335-Y	1.2305D+06	10	20-Y
2.7009D+03	639	289-Y	8.8502D+05	57	37-Y
2.7216D+03	749	329-Y	8.7763D+05	51	35-Y
2.8194D+03	573	265-Y	8.1049D+05	60	38-Y
3.0149D+03	664	298-Y	7.4085D+05	54	36-Y
3.0591D+03	730	322-Y	7.2247D+05	48	34-Y
3.0994D+03	87	48-Y	7.2240D+05	2	17-Y
3.1392D+03	750	329-Z	7.2226D+05	21	24-Y
3.1832D+03	685	306-X	6.8060D+05	63	39-Y
3.2086D+03	640	289-Z	5.2473D+05	101	53-Y
3.2683D+03	683	305-Y	5.2388D+05	6	19-X
3.2951D+03	708	314-Y	5.2112D+05	107	55-Y
3.3715D+03	776	339-Y	5.2107D+05	17	22-Z
3.4073D+03	729	322-X	5.2013D+05	3	18-X
3.4101D+03	722	319-Y	5.1868D+05	20	23-Z

15:55:10 (CP 4.51 485.98) End Of Decomposition
15:55:10 (CP 0.10 486.08) Begin Contact Force Iteration
15:55:28 (CP 10.69 496.77) Contact force convergence ratio: 0.002030892

I-DEAS Master Series 5: Model Solution Nonlinear Solver
29-Apr-99 15:55:28 PAGE 11

MODEL_SOLUTION_SOLVE

15:55:29 (CP 0.23 497.00) ----- End of Iteration -----
15:55:29 (CP 0.02 497.02)
15:55:30 (CP 1.02 498.04) Stiffness Parameter for Iteration : 0.01068139
15:55:30 (CP 0.42 498.46) Convergence Statistics
15:55:31 (CP 0.64 499.10) Energy Convergence Ratio: 8.344079E-06
15:55:31 (CP 0.20 499.30)
15:55:31 (CP 0.02 499.32) Equilibrium Iteration Number: 9
15:55:31 (CP 0.03 499.35)
15:55:32 (CP 0.01 499.36) ----- Begin Iteration -----
15:55:32 (CP 0.13 499.49) Form Contact Status
15:55:32 (CP 0.37 499.86) Number of contact status changes: 1
15:55:32 (CP 0.03 499.89) Number of inactive contacts: 91
15:55:32 (CP 0.02 499.91) Number of active open contacts: 0
15:55:33 (CP 0.03 499.94) Number of sticking contacts: 0
15:55:33 (CP 0.03 499.97) Number of sliding contacts: 49
15:55:36 (CP 0.76 500.73) Begin Stiffness Matrix Formation
15:55:46 (CP 6.39 507.12) Begin External Loads Formation
15:55:47 (CP 0.65 507.77) External Loads Formation Complete
15:55:48 (CP 0.39 508.16) Begin Internal Force Formation
15:55:51 (CP 2.55 510.71) Internal Force Formation Complete
15:55:51 (CP 0.05 510.76) Begin Stress Stiffness Matrix Formation
15:55:56 (CP 2.19 512.95) Begin Stiffness Matrix Partitioning
15:56:01 (CP 2.67 515.62) Contact Stiffness Partitions Formed
15:56:01 (CP 0.02 515.64) Stiffness Matrix Formation Complete
TOTAL VIRTUAL MEMORY SPECIFIED = 185 MB
PERCENT ALLOCATED TO APPLICATION MEMORY = 64 %
MEMORY ALLOCATED FOR SPARSE MATRIX SOLVER = 29 MB
MEMORY USED BY SPARSE MATRIX SOLVER = 6 MB
15:56:03 (CP 1.64 517.28) Sparse solve will be done in-memory
15:56:04 (CP 0.62 517.90) Est. decomp time = 7 cpu seconds
15:56:04 (CP 0.08 517.98) Begin Decomposition

SIZE OF SCRATCH FILES = 1 MB

CHOLESKY DECOMPOSITION STATISTICS:

SINGULARITY CRITERIA = 1.0E-14

NUMBER OF EQUATIONS = 2587

MINIMUM			MAXIMUM		
CHOLESKY EQUATION PIVOTS	EQUATION NUMBER	NODE AND DIRECTION	CHOLESKY EQUATION PIVOTS	EQUATION NUMBER	NODE AND DIRECTION

1.2966D+03	796	370-Y	1.3401D+06	13	21-Y
1.7906D+03	774	338-Y	1.3320D+06	16	22-Y
2.3054D+03	793	345-Y	1.3308D+06	7	19-Y
2.3146D+03	485	233-Y	1.2652D+06	4	18-Y
2.5449D+03	727	321-Y	1.2618D+06	19	23-Y
2.5569D+03	766	335-Y	1.2305D+06	10	20-Y
2.7009D+03	639	289-Y	8.8502D+05	57	37-Y
2.7215D+03	749	329-Y	8.7763D+05	51	35-Y
2.8194D+03	573	265-Y	8.1049D+05	60	38-Y
3.0149D+03	664	298-Y	7.4085D+05	54	36-Y
3.0590D+03	730	322-Y	7.2247D+05	48	34-Y
3.0994D+03	87	48-Y	7.2240D+05	2	17-Y
3.1391D+03	750	329-Z	7.2226D+05	21	24-Y
3.1831D+03	685	306-X	6.8060D+05	63	39-Y
3.2086D+03	640	289-Z	5.2473D+05	101	53-Y
3.2683D+03	683	305-Y	5.2388D+05	6	19-X
3.2951D+03	708	314-Y	5.2112D+05	107	55-Y

I-DEAS Master Series 5: Model Solution Nonlinear Solver

29-Apr-99

15:56:09

PAGE 12

MODEL_SOLUTION_SOLVE

3.3711D+03	776	339-Y	5.2107D+05	17	22-Z
3.4071D+03	729	322-X	5.2013D+05	3	18-X
3.4100D+03	722	319-Y	5.1868D+05	20	23-Z
15:56:09 (CP	4.53	522.51)	End Of Decomposition		
15:56:09 (CP	0.08	522.59)	Begin Contact Force Iteration		
15:56:22 (CP	10.49	533.08)	Contact force convergence ratio: 0.001410243		
15:56:23 (CP	0.19	533.27)	----- End of Iteration -----		
15:56:23 (CP	0.03	533.30)			
15:56:24 (CP	0.98	534.28)	Stiffness Parameter for Iteration : 0.01068095		
15:56:24 (CP	0.41	534.69)	Convergence Statistics		
15:56:25 (CP	0.60	535.29)	Energy Convergence Ratio: 0.00002272078		
15:56:25 (CP	0.19	535.48)			
15:56:25 (CP	0.01	535.49)	Equilibrium Iteration Number: 10		
15:56:26 (CP	0.03	535.52)			
15:56:26 (CP	0.02	535.54)	----- Begin Iteration -----		
15:56:26 (CP	0.17	535.71)	Form Contact Status		
15:56:26 (CP	0.37	536.08)	Number of contact status changes: 0		
15:56:26 (CP	0.03	536.11)	Number of inactive contacts: 91		
15:56:26 (CP	0.01	536.12)	Number of active open contacts: 0		
15:56:27 (CP	0.02	536.14)	Number of sticking contacts: 0		
15:56:27 (CP	0.03	536.17)	Number of sliding contacts: 49		
15:56:29 (CP	0.70	536.87)	Begin Stiffness Matrix Formation		
15:56:37 (CP	6.33	543.20)	Begin External Loads Formation		
15:56:38 (CP	0.69	543.89)	External Loads Formation Complete		

15:56:39 (CP 0.38 544.27) Begin Internal Force Formation
 15:56:42 (CP 2.50 546.77) Internal Force Formation Complete
 15:56:42 (CP 0.03 546.80) Begin Stress Stiffness Matrix Formation
 15:56:47 (CP 2.17 548.97) Begin Stiffness Matrix Partitioning
 15:56:51 (CP 2.64 551.61) Contact Stiffness Partitions Formed
 15:56:52 (CP 0.02 551.63) Stiffness Matrix Formation Complete
 TOTAL VIRTUAL MEMORY SPECIFIED = 185 MB
 PERCENT ALLOCATED TO APPLICATION MEMORY = 64 %
 MEMORY ALLOCATED FOR SPARSE MATRIX SOLVER = 29 MB
 MEMORY USED BY SPARSE MATRIX SOLVER = 6 MB
 15:56:54 (CP 1.64 553.27) Sparse solve will be done in-memory
 15:56:54 (CP 0.61 553.88) Est. decomp time = 7 cpu seconds
 15:56:54 (CP 0.09 553.97) Begin Decomposition
 SIZE OF SCRATCH FILES = 1 MB

CHOLESKY DECOMPOSITION STATISTICS:

SINGULARITY CRITERIA = 1.0E-14

NUMBER OF EQUATIONS = 2587

MINIMUM			MAXIMUM		
CHOLESKY	EQUATION	NODE AND	CHOLESKY	EQUATION	NODE AND
PIVCTS	NUMBER	DIRECTION	PIVOTS	NUMBER	DIRECTION

1.2966D+03	796	370-Y	1.3401D+06	13	21-Y
1.7905D+03	774	338-Y	1.3320D+06	16	22-Y
2.3053D+03	793	345-Y	1.3308D+06	7	19-Y
2.3146D+03	485	233-Y	1.2652D+06	4	18-Y
2.5449D+03	727	321-Y	1.2618D+06	19	23-Y
2.5569D+03	766	335-Y	1.2305D+06	10	20-Y
2.7009D+03	639	289-Y	8.8502D+05	57	37-Y
2.7215D+03	749	329-Y	8.7763D+05	51	35-Y
2.8194D+03	573	265-Y	8.1049D+05	60	38-Y
3.0149D+03	664	298-Y	7.4085D+05	54	36-Y
3.0590D+03	730	322-Y	7.2247D+05	48	34-Y

I-DEAS Master Series 5: Model Solution Nonlinear Solver

29-Apr-99 15:56:59 PAGE 13

MODEL_SOLUTION_SOLVE

3.0994D+03	87	48-Y	7.2240D+05	2	17-Y
3.1391D+03	750	329-Z	7.2226D+05	21	24-Y
3.1831D+03	685	306-X	6.8060D+05	63	39-Y
3.2086D+03	640	289-Z	5.2473D+05	101	53-Y
3.2683D+03	683	305-Y	5.2388D+05	6	19-X
3.2951D+03	708	314-Y	5.2112D+05	107	55-Y
3.3709D+03	776	339-Y	5.2107D+05	17	22-Z
3.4071D+03	729	322-X	5.2013D+05	3	18-X
3.4100D+03	722	319-Y	5.1868D+05	20	23-Z
15:56:59 (CP 4.58 558.55)	End Of Decomposition				
15:57:00 (CP 0.11 558.66)	Begin Contact Force Iteration				
15:57:13 (CP 10.66 569.32)	Contact force convergence ratio: 0.001109527				
15:57:13 (CP 0.21 569.53)	----- End of Iteration -----				
15:57:13 (CP 0.02 569.55)					
15:57:14 (CP 1.01 570.56)	Stiffness Parameter for Iteration : 0.01068075				
15:57:15 (CP 0.40 570.96)	Convergence Statistics				
15:57:16 (CP 0.63 571.59)	Energy Convergence Ratio: 0.00002626706				

15:57:18 (CP 2.54 574.13)
15:57:18 (CP 0.01 574.14) Displacements Obtained
15:57:19 (CP 0.01 574.15)

NET APPLIED LOAD FOR LOAD SET 9 - P40000

FX = -4.58057D-09, FY = -1.75178D+03, FZ = 7.77074D-09
MX = 2.51659D+03, MY = 2.74037D-04, MZ = -2.51663D+03
MOMENTS TAKEN ABOUT THE ORIGIN

NET REACTION FORCE FOR LOAD SET 9 - P40000

FX = -1.08240D-08, FY = 1.75178D+03, FZ = 1.55099D-08
MX = -2.52306D+03, MY = -1.66481D-04, MZ = 2.52315D+03
MOMENTS TAKEN ABOUT THE ORIGIN

SIZE OF HYPERMATRIX FILE = 24 MB

15:57:32 (CP 7.35 581.50) END OF ANALYSIS

GLOSSARY

Subcutaneous	Being, living, used, or made under the skin
Auricular	An epithelial parenchymatous cell of the liver
Parenchyma	The essential and distinctive tissue of an organ or an abnormal growth as distinguished from its supportive framework
Laparotomy	Surgical section of the abdominal wall
Lesions	Abnormal change in structure of an organ or part due to injury or disease
Laparoscopic	A fiber optic instrument inserted through an incision in the abdominal wall and used to examine visually the interior of the peritoneal cavity
Hematocrit	The ratio of the volume of packed red blood cells to the volume of whole blood
Histologic	Tissue structure or organization
Meningiomas	A slow-growing encapsulated tumor arising from the meninges and often causing damage by pressing upon the brain and adjacent parts.
Perineal	The area between the anus and the posterior part of the external genitalia
Angioplasty	Surgical repair of a blood vessel; especially: BALLOON ANGIOPLASTY
Mongrel	An individual resulting from the interbreeding of diverse breeds or strains
Thrombus	A clot of blood formed within a blood vessel and remaining attached to its place of origin
Parenchymatous	The essential and distinctive tissue of an organ or an abnormal growth as distinguished from its

REFERENCES

1. M. Alitavoli, J. A. McGeough, 1998, "An Expert Process Planning System for Meat Cutting by High Pressure Water-Jet," *Journal of Material Processing Technology*, vol. 76, pp. 146-152.
2. S. M. Arif, 1997, "Finite Element Analysis of Skin Injuries by Water Jet Cutting" Master Thesis, Department of Industrial and Manufacturing Engineering, New Jersey Institute of Technology, Newark, New Jersey.
3. C. P. Artz, D. R. Yarbrough 3rd, 1973, "Major body burn," *Journal of the American Medical Association*, vol. 223(12), pp. 1355-1357.
4. K. J. Bathe, 1996, *Finite Element Procedures*, Prentice Hall, Upper Saddle River, New Jersey.
5. A. Cuschieri, 1994, "Experimental evaluation of water-jet dissection in endoscopic surgery," *Endoscopic Surgery Allied Technology*, vol. 2(3-4), pp. 202-204.
6. E. Gordon, B. Parolini, M. Abelson 1998, "Principles and microscopic confirmation of surface quality of two new waterjet-based microkeratomes," *Journal of Refractive Surgery*, vol. 14(3), pp. 338-345.
7. R. L. Harvey, D. A. Ashley, L. Yates, M. L. Dalton, M. M. Solis, 1996, "Major vascular injury from high-pressure water jet," *Journal of Trauma*, vol. 40(1), pp.165-167.
8. J. Hubert, E. Mourey, J. M. Suty, A. Coissard, J. Floquet, P. Mangin 1996, "Water-jet dissection in renal surgery: experimental study of a new device in the pig," *Urological Research*, vol. 24(6), pp. 355-359.
9. S. D. Kirby, B. Wang, C. W. Solomon To, H. B. Lampe, 1998, "Nonlinear, Three-Dimensional Finite-Element Model of Skin Biomechanics," *The Journal of Orolaryngology*, vol. 27, pp. 153-160.
10. M. Kobayashi, S. Sawada, N. Tanigawa, T. Senda, Y. Okuda, 1995, "Water jet angioplasty--an experimental study," *Acta Radiologica*, vol. 36(4), pp. 453-456.
11. W. F. Larrabee jr., J. A. Galt, 1997, "A Finite Element Model of Skin Deformation III. The Finite Element Model," *Laryngoscope*, vol. 96, pp. 413-419.
12. M. H. Lawry, *I-DEAS Master Series Student Guide*, Structural Dynamics Research Corporation, Millford, Ohio.
13. D. N. Papachristou, R. Barters, 1982, "Resection of the liver with a water jet," *British Journal of Surgery*, vol.69(2), pp.93-94.

14. R. D. Penchev, K. T. Kjossev, J. E. Losanoff, 1997, "*Application of a new water jet apparatus in open hepatobiliary surgery: hepatic resection, cholecystectomy, common bile duct lavage,*" *International Surgery*, vol. 82(2) pp. 182-186.
15. H. G. Rau, G. Meyer, K. W. Jauch, T. U. Cohnert, E. Buttler, F. W. Schildberg, 1996, "*Liver resection with the water jet: conventional and laparoscopic surgery,*" *Chirurg*, vol. 67(5), pp. 546-551.
16. S. A. Ray, R. M. Rainsbury, 1992, "*High pressure industrial steam washer injury resulting in digital amputation,*" *Burns*, vol. 18(3), pp. 256.
17. M. O. Schurr, M. Wehrmann, W. Kunert, A. Melzer, M. M. Lirici, R. Trapp, E 1995. Kanehira, G. Buess 1994, "*Histologic effects of different technologies for dissection in endoscopic surgery: Nd:YAG laser high frequency and water-jet,*" *Endoscopic Surgery Allied Technology*, vol. 2(3-4) pp.195-201.
18. O. M. Schob, R. B. Schlumpf, G. K. Uhlschmid, C. Rausis, M. Spiess, F. Largiader, "*The multimodal water jet dissector--a technology for laparoscopic liver surgery,*" *Endoscopic Surgery Allied Technology*, vol. 2(6), pp. 311-314.
19. R. Siegert, J. Danter, V. Jurk, R. Eggers, S. Kruger, 1998, "*Dermal microvasculature and tissue selective thinning techniques (ultrasound and water-jet) of short-time expanded skin in dogs,*" *European archives of oto-rhino-laryngology*, vol. 255(6), pp. 325-30.
20. R. Skalak, S. Chien, 1987, *Handbook of Bioengineering*, McGraw-Hill. Inc., New York.
21. N. Sohn and M. A. Weinstein, 1977, "*Unhealed perineal wound: lavage with a pulsating water jet,*" *American Journal of Surgery*, vol.134(3), pp.426-427.
22. A. J. Terzis, G. Nowak, O. Rentzsch, H. Arnold, J. Diebold, G. Baretton, 1989, "*A new system for cutting brain tissue preserving vessels: water jet cutting,*" *British Journal of Neurosurgery*, vol. 3(30), pp. 361-366.
23. R. A. Tikhomirov, V. F. Bahanin, E.N. Petukhov, I. D. Starikov, V. A. Kovalev, 1992 "*High-Pressure Jetcutting*", ASME Press, NY.
24. S. Toth, J. Vajda, E. Pasztor, Z. Toth, 1987, "*Separation of the tumor and brain surface by "water jet" in cases of meningiomas,*" *Journal of Neuro-oncology*, vol. 5(2), pp. 117-124.
25. Y. Une Y, J. Uchino, T. Shimamura, T. Kamiyama, I. Saiki, " 1996, *Water jet scalpel for liver resection in hepatocellular carcinoma with or without cirrhosis,*" *International Surgery*, vol. 81(1), pp. 45-48.
26. C. L. Yarbrough, 1981, "*Infection control series: I. Skin manifestations of selected infectious diseases,*" *West Virginia Medical Journal*, vol. 77(4), pp. 79-82.